RESEARCH ARTICLE

Geoarchaeology An International Journal   WILEY

The micromorphology of loess-paleosol sequences in central Alaska: A new perspective on soil formation and landscape evolution since the Late Glacial period (c. 16,000 cal yr BP to present)

Jennifer Kielhofer[1] | Christopher Miller[2,3] | Joshua Reuther[4] |
Charles Holmes[5] | Ben Potter[6] | François Lanoë[7] | Julie Esdale[8] | Barbara Crass[4]

[1]Department of Geosciences, University of Arizona, Tucson, Arizona

[2]Institute for Archaeological Sciences & Senckenberg Center for Human Evolution and Paleoenvironment, University of Tübingen, Tübingen, Germany

[3]SFF Centre for Early Sapiens Behaviour (SapienCE), University of Bergen, Norway

[4]Museum of the North, University of Alaska, Fairbanks, Alaska

[5]Department of Anthropology, University of Alaska, Fairbanks, Alaska

[6]Arctic Studies Center, Liaocheng University, Liaocheng, China

[7]Bureau of Applied Research in Anthropology, University of Arizona, Tucson, Arizona

[8]Center for Environmental Management of Military Lands, Colorado State University, Fort Collins, Colorado

Correspondence
Jennifer Kielhofer, Department of Geosciences, University of Arizona, 1040 E 4th St, Tucson, AZ 85721.
Email: jkielhofer@email.arizona.edu

Abstract

The middle Tanana Valley of central Alaska contains a well-preserved record of human occupation and paleoenvironmental change since the Late Glacial period (c. 16,000 cal yr BP) and is a critical region for understanding human dispersal into the Americas. Micromorphology analysis of soils and sediments from six archaeological sites yields valuable information about soil formation processes and landscape evolution during the Late Glacial and into the Holocene. At the macroscale, site stratigraphies are very similar, and thin organic-rich layers (locally known as "stringers") are commonly interpreted as buried soils. However, at the microscale, these layers exhibit significant differences in the degree of bioturbation, organic matter humification, and boundary abruptness, indicating that pedogenesis was not the sole process at every site. In this way, our microscale analysis addresses issues of equifinality related to site formation interpretations, a persistent problem with subarctic and high-latitude stratigraphy. Additionally, this study reveals a certain level of landform and landscape instability within a broader trend of regional increases in pedogenesis and vegetation coverage, adding to the existing model of heterogeneity across this subarctic landscape. Here we demonstrate the utility of micromorphology to test field interpretations and improve models of Late Glacial landscape evolution in high-latitude contexts.

KEYWORDS
central Alaska, Holocene, Late Pleistocene, loess-paleosol stratigraphy, micromorphology, subarctic

1 | INTRODUCTION

Loess-paleosol sequences in the middle Tanana Valley (mTV) in central Alaska contain some of the oldest, firmly dated archaeological sites in North America (Late Glacial, c. 15,000-13,000 cal yr BP), which are considered key for understanding the initial entry of humans into the Americas (Hoffecker & Elias, 2007; Potter, Holmes,

& Yesner, 2013; Reuther et al., 2016). At these sites, Late Glacial archaeological deposits are commonly associated with thin (mm-to-cm scale), dark brown "stringers" (a local term) enriched in organic material (Figure 1; Dilley, 1998; Reuther, 2013). Similar stringers are noted at archaeological sites in neighboring regions (Graf et al., 2015; Thorson & Hamilton, 1977). Previous geoarchaeological work interprets these stringers as weakly developed buried A horizons,
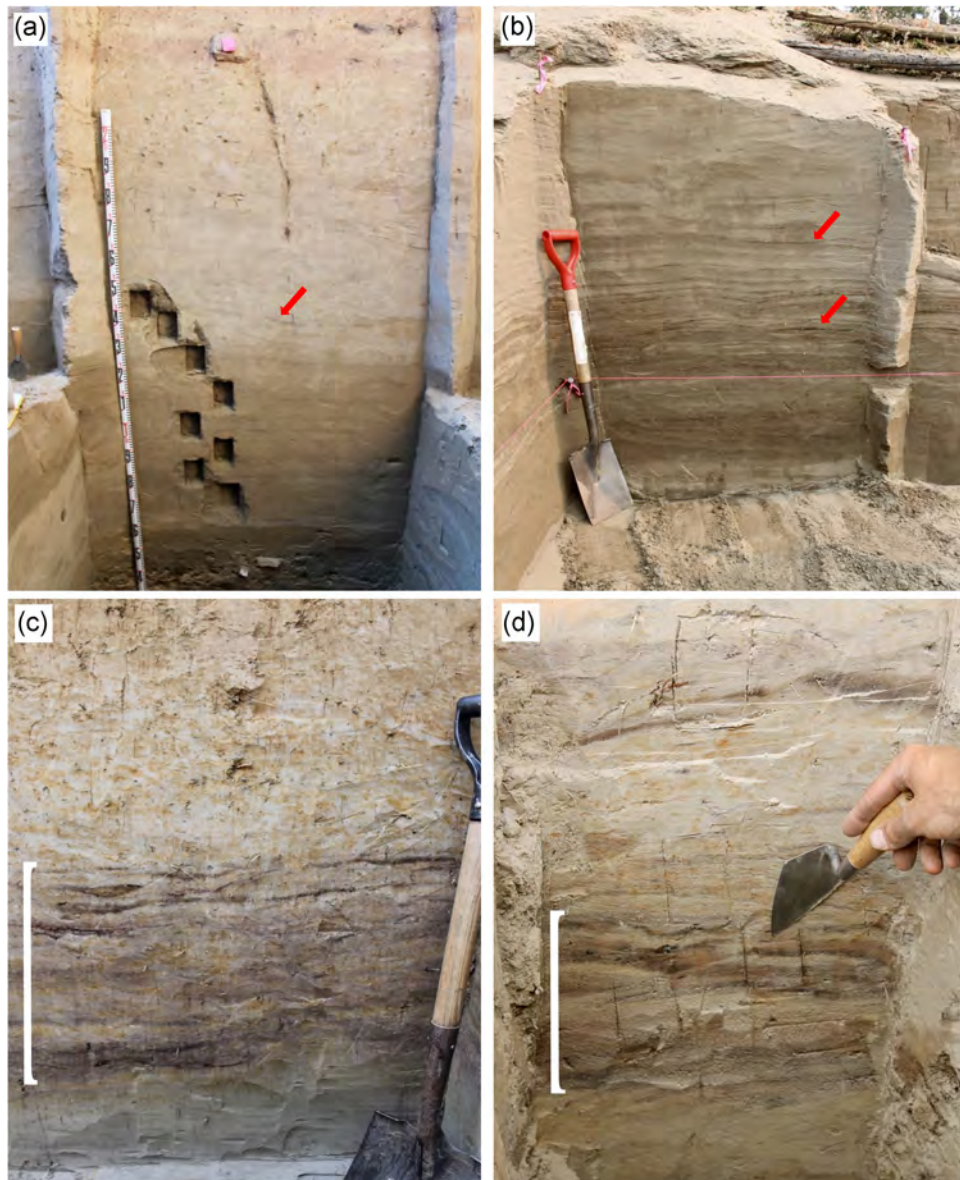
FIGURE 1 Overview of "stringer" features in the field, highlighting broad similarity in thickness, color, and overall macroscale appearance. Red arrows in (a) and (b) point toward examples of stringers at each site, and the white brackets in (c) and (d) indicate thicker areas with multiple stringers. (a) Weak stringers in Late Glacial sediments at the Cook site. Micromorphology samples are shown in the exposure wall. There is a tape for scale. (b) Numerous stringers in the north profile wall of an excavation unit at Keystone Dune. There is a shovel for scale. (c) A series of more prominent stringers at Mead. These stringers make up two paleosol complexes, known as the Upper and Lower Paleosol Complex. There is a shovel for scale. (d) A series of more prominent stringers, designated as Pedocomplex 1, at Hurricane Bluff. There is a trowel for scale [Color figure can be viewed at wileyonlinelibrary.com]

implying some degree of surface landscape stability during early human occupation (Figure 1a,b; Dilley, 1998; Graf et al., 2017; Reuther, 2013). A few sites contain thicker packages of stringers and organic enrichment described as pedocomplexes or paleosol complexes (Figure 1c,d; Potter et al., 2013; Reuther, 2013). Although commonly interpreted as soil horizons, these stringers are unusual when compared to many typical soils around the world and can be difficult to describe and sample in the field, which creates challenges for understanding soil and site formation processes.

Micromorphological analysis provides a valuable tool for resolving the nature of these Alaskan stringers, which is central for interpreting the formation history and paleoenvironmental context of early archaeological sites. Micromorphology, the petrographic analysis of in situ structures within sediments and soils, is a powerful technique for studying fine-scale features of geological and archaeological deposits that are often unobservable in the field and/or destroyed by methods that rely on bulk samples (Courty, 2001; Courty, Goldberg, & Macphail, 1989). This method provides a quick and inexpensive way to test field

interpretations, preserving intact "microfacies" and microscale features of stratigraphy. In interior Alaska, micromorphology has been used to study the stratigraphy of single sites (Blong & DiPietro, 2014; Gilbert, 2011; Graf et al., 2017, 2015; Josephs, 2010); however, this technique has yet to be applied across multiple sites within the same region for comparative purposes.

Our main goal was to study these stringers and paleosol complexes using micromorphology and test the hypothesis that dark brown stringers represent buried soils and pedogenesis (i.e., soil formation) at multiple sites. Specific research questions include: (a) Are these layers buried soils, or do they reflect nonpedogenic geomorphological processes?; (b) If these stringers and paleosol complexes are buried soils, which pedogenic process(es) influenced their formation? Do these pedogenic processes differ from site to site? Why do these stringers look so different from "typical" buried soils?; (c) Do we see any evidence of stratigraphic disturbance or pedoturbation in these layers?; (d) What can micromorphology reveal about site formation histories?; and finally, (e) Do soil and sediment characteristics at the microscale provide new insight on landscape evolution in interior Alaska during the Late Glacial and Holocene?

Resolving the nature of these stringers as buried soils holds great significance for understanding past landscapes at our study sites. If our stringers are entirely pedogenic, their presence implies periods of landscape stability (e.g., lack of sediment deposition, or insufficient deposition to outpace soil formation) and a more stable surface for early human occupation, whereas depositional units signify a relatively unstable and dynamic landscape. By addressing these questions, we shed light on microscale formation mechanisms of Late Glacial "stringers" and landscape processes at our sites, with implications for improving current models of landscape change and human paleoecology in eastern Beringia.

2 | REGIONAL SETTING

The mTV is a lowland basin in interior Alaska, bordered by the Alaska Range to the south and the Yukon Tanana Uplands to the north and east (Figure 2a). Most of our sites are located in the Shaw Creek Flats (SCF), a low-lying alluvial plain within the mTV lowlands and adjacent to the Yukon-Tanana Uplands. The mTV was never completely
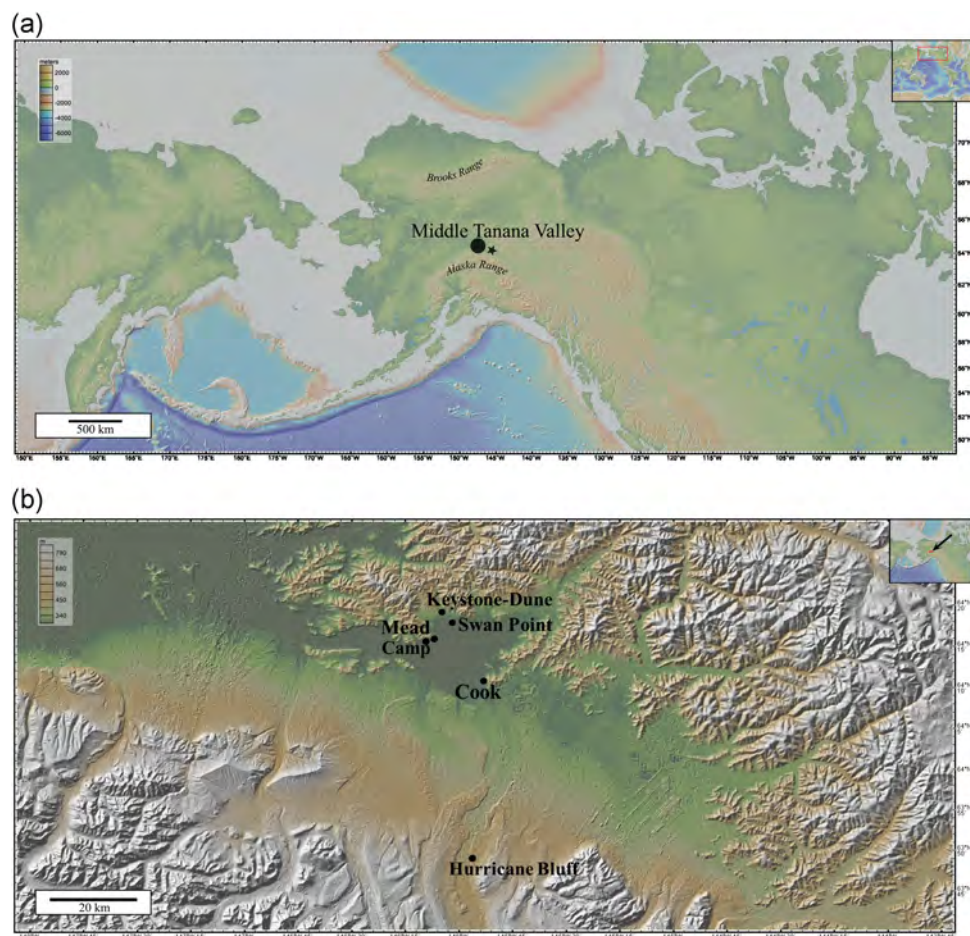
FIGURE 2 Global multiresolution topography map of our study region and study sites, using the GeoMapApp software program. (a) Overview of the middle Tanana Valley (our wider study region) in central Alaska. Major mountain ranges are labeled. (b) Locations of our six site study sites. Five sites (Mead, Camp, Swan Point, Keystone Dune, and Cook) are located in the middle Tanana Valley, while Hurricane Bluff is located in the neighboring Delta River Valley. *The location of the Shaw Creek Flats area [Color figure can be viewed at wileyonlinelibrary.com]

glaciated, however the region's late Quaternary landscape evolution was significantly shaped by glacial processes (Péwé & Reger, 1983; Reger & Solie, 2008; Ten Brink & Waythomas, 1980). SCF formed through aggradation of the Tanana River from Donnelly glacial outwash (c. 25,000-16,000 cal yr BP; Matmon, Briner, Carver, Bierman, & Finkel, 2010; Reger & Péwé, 2002; Reger, Stevens, & Solie, 2008; Reuther et al., 2016). The majority of loess that blankets upland terraces and bluffs across SCF is related to the end of the Donnelly glaciation and thereafter into the Late Glacial and Holocene (Dilley, 1998; Muhs et al., 2003; Reuther, 2013). During the Donnelly glaciation, the region may have served as a refugium for faunal and floral communities (Guthrie, 1990).

Modern soil development in SCF is controlled by several factors, including soil temperature, topography, landscape disturbance, vegetation, drainage, permafrost extent and depth, and the sedimentation and/or erosion rate (Ping et al., 2005; Reuther, 2013; Rieger, Schoephorster, & Furbush, 1979). Organic-rich soils and peats (Histosols) develop in areas of water saturation, including poorly drained, low-lying zones in river valleys or alluvial flats, swales or depressions on south-facing slopes, or north-facing slopes with ice-rich sediments. Weakly or moderately developed soils (Entisols and Inceptisols, or less commonly immature Spodosols) tend to form in well-drained settings and/or on south-facing slopes.

Over the past few decades, SCF has been of great interest to Alaskan and North American archaeologists. Several well-stratified, multicomponent sites have been discovered in aeolian deposits on elevated landforms, such as sand dunes, bluff edges, and bedrock knolls. These sites are firmly dated between c. 15,000 and 13,000 cal yr BP and offer a window into some of North America's earliest occupations (Hoffecker & Elias, 2007; Potter, 2009; Potter et al., 2013). The best-known sites in the SCF include Swan Point, Mead, and Broken Mammoth, which are located within 10 km of each other and contain Bølling-Allerød (c. 14,000–12,900 cal yr BP) and Younger Dryas (c. 12,900–11,600 cal yr BP) occupations (Dilley, 1998; Holmes, 2001; Lanoë & Holmes, 2016; Potter et al., 2013; Yesner, 1996). Late Glacial occupations at lesser known SCF sites include Bachner, Cook, Keystone Dune, and Holzman South (Lanoë, Reuther, Holloway, Holmes, & Kielhofer, 2018; Reuther, 2013; Reuther et al., 2016; Wooller et al., 2012; Wygal, Krasinski, Holmes, & Crass, 2018). Other important Late Glacial and Early Holocene components outside of the SCF include the Gerstle River Quarry, Delta River Overlook, Hurricane Bluff, and Upward Sun River sites (Potter, 2009; Potter, Bowers, Reuther, & Mason, 2007; Potter, Irish, Reuther, Gelvin-Reymiller, & Holliday, 2011; Potter et al., 2018).

2.1 | Study localities

Our analysis includes samples from Swan Point, Mead, Camp, Keystone Dune, Cook, and Hurricane Bluff (Figure 2b). Here we summarize previous archaeological, stratigraphic, and chronological work (Figure 3 and Table S1). The Supporting Information Materials contain additional information about lithostratigraphy, pedostratigraphy, geochronology, and micromorphology.

2.1.1 | Swan Point site

Swan Point (XBD-156) sits on an isolated bedrock knoll along the northern margin of SCF. This knoll rises c. 30 m above the surrounding lowlands and overlooks stabilized sand dunes, thaw ponds, and marshlands along Shaw Creek (Dilley, 1998). The site has been intermittently excavated (65 m² total) since its discovery in 1991 (Figure S1). Lithostratigraphy consists of sands and silts c. 80–100 cm thick at the knoll's crest (Figures 3, S2, and S3; Dilley, 1998; Holmes, 2001, 2011). Previous researchers describe stringers of charcoal fragments and diffuse organic material within the aeolian sediments as discontinuous buried soils (Dilley, 1998; Holmes, 2001, 2011). The lowest paleosols, 2Ab and 2C, are loamy fine sands (10YR 3/2 and 2.5YR 5/2) with single grain structure and little pedogenic iron, aluminum, or carbonate (Dilley, 1998). In 2016, our hand coring and excavation in a $1 \times 1\,m^2$ test pit, ~15 m west of the main excavation, revealed variation in deposit thickness and expression of stratigraphic units across the landform (Figures S4 and S5).

The oldest archaeological occupation, Cultural Zone 4b (CZ4b), dates to ~12,060 ± 70 ^{14}C yr BP (14,090–13,750 cal yr BP), which ties initial occupation to the early Bølling-Allerød (Hirasawa & Holmes, 2017; Holmes, 2011). In CZ4b, there are abundant microblades and burins, and faunal remains include large herbivores (e.g., mammoth, horse, bison, and caribou), lagomorphs, rodents, and birds (especially waterfowl; Gómez Coutouly & Holmes, 2018; Hirasawa & Holmes, 2017; Lanoë & Holmes, 2016). Based on prevalent mammoth (*Mammuthus primigenius*) ivory and tusks, Swan Point may have been a specialized workshop for organic-based tools (Lanoë & Holmes, 2016). CZ3 has a mean date of 10,080 ± 40 ^{14}C yr BP (11,820–11,400 cal yr BP), suggesting Younger Dryas to Early Holocene occupation (Holmes, 2011; Potter et al., 2013). This component contains microblades, but bifacial tools are more prevalent. The faunal assemblage is less diverse than that of CZ4, dominated by large ungulates (i.e., bison, moose, and wapiti; Holmes, 2011; Lanoë, 2018; Potter et al., 2013).

2.1.2 | Mead site

The Mead site (XBD-071) is situated at the edge of a bedrock terrace along the Shaw Creek Bluff (Péwé, 1965; Potter et al., 2013), c. 10 m above the SCF. The site has a southeastern aspect. Cliffhead sands and overlying loess cap the bedrock terrace (Figure S6; Dilley, 1998; Potter, Gilbert, Holmes, & Crass, 2011). Loess depths are relatively constant (c. 2 m thick) across the terrace, with slightly thinner deposits (c. 1 m thick) near its edge. Cliffhead sands vary significantly in thickness across the landform, ranging from <50 cm thick near the terrace edge to >4 m thick c. 100 m upslope from the edge.
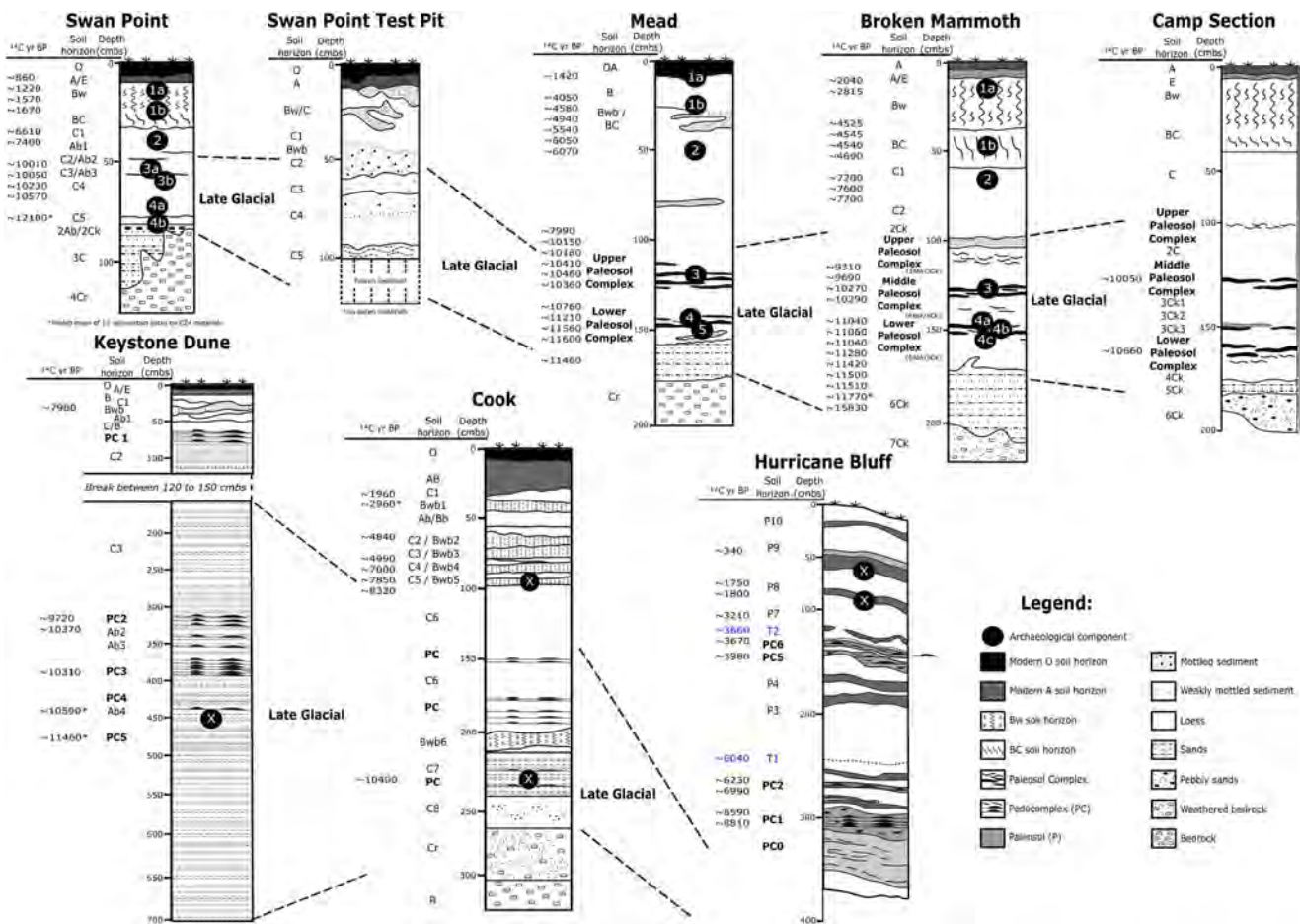
FIGURE 3 Stratigraphic sequences at our six study sites, showing radiocarbon dates, identified lithostratigraphic and pedostratigraphic units, soil horizon designations from the original stratigraphic work, and the depth of archaeological occupations. A "*" next to a date indicates that multiple dates were pooled and averaged. We also demarcate the correlation of Late Glacial units from site to site, highlighting the variability in local stratigraphy and local environments across the study region. Radiocarbon dates and stratigraphic profiles were compiled and/or modified from the following references: Swan Point—Holmes (2011); Mead—Holmes (2001), Potter et al. (2011), Potter et al. (2013); Broken Mammoth—Dilley (1998), Holmes (1996); Camp—Dilley (1998); Keystone Dune—Reuther (2013), Reuther et al. (2016); Cook—Reuther (2013); Hurricane Bluff—Reuther et al. (2018). Since the Potter et al. (2011) publication on Mead, two radiocarbon dates (>770 ± 40 and 7,620 ± 100) have been rejected and thus were removed from this figure. At Swan Point, 1,750 ± 80 and 4,260 ± 40 have also been rejected and thus were removed from this figure. Please see Table S2 for a complete list of dates and chronological information [Color figure can be viewed at wileyonlinelibrary.com]

Small-scale archaeological excavations took place in the 1990s with more extensive excavation occurring between 2009 and 2016. Archaeological excavations along the terrace total >128 m[2] and reveal a deeply buried multicomponent site (Potter et al., 2013). Mead is interpreted as a mixed foraging camp (Potter et al., 2013). Over 37 AMS radiocarbon dates temporally constrain the main excavation (Potter et al., 2013). The oldest cultural components, CZ5 and CZ4, are associated with the Lower Paleosol Complex. Radiocarbon dates of 11,460 ± 50 ^{14}C yr BP (13,430–13,190 cal yr BP) and 11,050 ± 40 ^{14}C yr BP (13,040–12,790 cal yr BP) bracket these cultural zones and suggest initial occupation during the Bølling–Allerød period (Potter et al., 2013). CZ5 and CZ4 assemblages consist of multiple hearth features, >1,500 lithic artifacts, and large faunal scatters (e.g., bison, wapiti, small game, and waterfowl; Potter et al., 2013; Potter, Gilbert et al., 2011). CZ3 is associated with the Upper Paleosol Complex.

This component consists of 10 hearths and >300 lithic artifacts, with a mean radiocarbon age of 10,270 ± 20 ^{14}C yr BP (12,140–11,950 cal yr BP; Potter et al., 2013; Potter, Gilbert, et al., 2011). Bison (Bison priscus) continue to dominate the faunal assemblage, although fish (Oncorhynchus sp.) notably first appear in CZ3 (Potter et al., 2013).

In 2008, excavation of a 1 × 2 m[2] test pit c. 100 m upslope (northwest) from the main excavation area revealed an anthropogenically undisturbed Late Glacial to Holocene stratigraphic sequence (Figure S7). Five radiocarbon ages from this test pit range between 12,760 and 11,620 cal yr BP (Table S2). Our micromorphology sampling focused on deposits in this test pit (Figures S8 and S9). Previous micromorphological analysis in the main excavation area indicates intensified pedogenesis under cooler climatic conditions during the Younger Dryas (Gilbert, 2011). Although intensified, pedogenesis at this time was still relatively weak, resulting in Ab

horizons with no evidence of weathering or B horizon formation (Gilbert, 2011).

2.1.3 | Camp section (comparable to the Broken Mammoth archaeological site)

Erosion has destabilized the well-known Broken Mammoth site (XBD-131) and prevented sampling for this study. Instead, we collected samples from the nearby Camp Section, a late Quaternary roadcut exposure correlated to Broken Mammoth (Figure S10; Dilley, 1998). Similar to the Mead site, Broken Mammoth and the Camp section are located along the Shaw Creek Bluff. The Camp section is south-facing and sits c. 300 m north of Broken Mammoth, c. 1 km southwest of Mead, and c. 7 km south-southwest of the Swan Point. The exposure is elevated c. 50 m above the Tanana River. The stratigraphic sequence consists of >2 m of well-drained fluvial, colluvial, and aeolian sediments overlying gneissic bedrock (Figures S10, S11, and S12; Dilley, 1998). There are three thicker buried soils in the aeolian section, which can be correlated to the Lower, Middle, and Upper Paleosol Complexes at Broken Mammoth (Figure S13; Dilley, 1998). Both the Lower and Middle Paleosol Complexes are 5–10 cm thick and consist of semicontinuous, undulating, dark brown (7.5YR 3/2 to 7.5YR 5/2) organic layers (Dilley, 1998). Camp paleosols show relatively weak development, although pedogenic carbonate features (e.g., root casts, thin horizontal laminations) appear common in the field (Dilley, 1998). The Lower Paleosol Complex is constrained by one AMS radiocarbon date of $10,660 \pm 80$ [14]C yr BP ($12,730$–$12,520$ cal yr BP), and the Middle Paleosol Complex by one AMS date of $10,050 \pm 95$ [14]C yr BP ($11,970$–$11,260$ cal yr BP; Figure S12; Dilley, 1998).

2.1.4 | Keystone Dune site

The Keystone Dune site (XBD-363) is located in the Rosa-Keystone Dune Field, which sits at the base of bedrock ridges at the northern and western extent of the SCF. The site has a southwestern aspect. Displaced artifacts from the site were initially discovered in 2008, following construction of the Pogo Mine Road and exposure of an erosional surface (Lanoë et al., 2018). Excavations totaling >22 m^2 were conducted in 2015 and 2016 and yielded hundreds of bone fragments, several lithic artifacts, and hearth features (Lanoë et al., 2018). This site is interpreted as a short-term hunting camp (Lanoë et al., 2018).

The stratigraphic sequence consists of aeolian sand, silt, and buried Entisols (Ab horizons) spanning the Late Glacial and Early Holocene (Figures S14 and S15; Reuther, 2013; Reuther et al., 2016). Pedocomplexes 4 and 5 reflect the earliest soil formation at the site. Both pedocomplexes consist of dark brown, fine sandy loams with weak iron oxidation and thin organic laminations (Reuther et al., 2016). A thicker (7–20 cm) buried Entisol, associated with the archaeological materials, separates these pedocomplexes. Large ungulate (in particular, wapiti [*Cervus elaphus*]) remains from Pedocomplex 5 yield an age of $11,470 \pm 40$ [14]C yr BP ($13,420$–$13,220$ cal yr BP), and hearth charcoal dates to $11,450 \pm 40$ [14]C yr BP ($13,410$–$13,190$ cal yr BP; Reuther et al., 2016). At least 16 buried soils and organic "stringers" overlie Pedocomplex 5, dating between $10,590 \pm 50$ [14]C yr BP ($12,690$–$12,510$ cal yr BP) and $9,720 \pm 50$ [14]C yr BP ($11,240$–$11,070$ cal yr BP; Reuther et al., 2016). Previous work describes these buried soils as thin (0.5–2 cm), weakly developed, black Entisols (Ab horizons; Reuther et al., 2016).

2.1.5 | Cook site

The Cook site (XBD-072) is located on the southeastern margin of SCF. The site sits on a ridgeline of bedrock hills that surround Quartz Lake and has a southwestern aspect (Reuther, 2013). The lithostratigraphy consists of weathered bedrock overlain by 3+ m of gravels and aeolian sand and silt deposits (Figures S16 and S17; Reuther, 2013). At least eight buried soils are observed within the aeolian sediments. Upper soils (Ab/Bb and Bwb horizons, 40–100 cmbs) are better developed and likely represent incipient forest soils, similar to those associated with poplar/aspen (*Populus*) and spruce (*Picea*) charcoal documented around the hills of Quartz Lake (Reuther, 2013). The earliest of these soils developed between $7,850 \pm 50$ [14]C yr BP ($8,790$–$8,540$ cal yr BP) and $7,000 \pm 60$ [14]C yr BP ($7,940$–$7,700$ cal yr BP; Reuther, 2013). These soils are associated with unidentified faunal remains and lithic artifacts (Reuther, 2013). Bone collagen from faunal remains discovered at 95 cmbs yielded a radiocarbon date of $8,320 \pm 30$ [14]C yr BP ($9,440$-$9,260$ cal yr BP; Table S2). Soils in the lower sequence (between 100 and 245 cmbs) appear faint and weakly developed (Ab and Abk horizons). The deepest pedocomplex consists of two thin (<1 cm), weakly developed organic and carbonate-rich silt loams (Reuther, 2013). Faunal remains from the deepest cultural component (~195 cmbs) date to $10,400 \pm 60$ [14]C yr BP ($12,440$–$12,040$ cal yr BP; Lanoë, Reuther, & Holmes, 2018).

2.1.6 | Hurricane Bluff site

The Hurricane Bluff site (XBD-838), located in the neighboring Delta River Valley (DRV) ~50 km southeast of the SCF area, serves as a useful interregional comparison to SCF sequences. Hurricane Bluff is situated on a glaciofluvial terrace with a southern aspect, 140 m from the Delta River Overlook site (Péwé & Reger, 1993; Potter et al., 2018). The site sits ~45 m above the river floodplain and overlooks the Delta River. Aeolian and silt deposits overlie ~360 cm of glaciofluvial sediments on the terrace (Figures S18 and S19; Potter et al., 2007; Reuther, Potter, Mulliken, & Kielhofer, 2018). Unit 2, a thick package of aeolian sediment (c. 320 cm), contains buried soils or buried soil complexes (pedocomplexes), two tephras, and archaeological material (Reuther et al., 2018). Twelve total soil pedocomplexes and paleosols have been identified at the site and classified as Entisols and Inceptisols. Charcoal from the lowest ABwb horizon in Pedocomplex 1 (Unit 2) yielded ages of $8,590 \pm 30$ [14]C yr BP ($9,600$–$9,520$ cal yr BP) and $8,810 \pm 60$ [14]C yr BP

(10,160–9,660 cal yr BP; Reuther et al., 2018). Charcoal from Pedocomplex 5 and Paleosol 7 dates to 3,980 ± 30 ^{14}C yr BP (4,530–4,410 cal yr BP) and 3,210 ± 30 ^{14}C yr BP (3,480–3,370 cal yr BP), respectively (Reuther et al., 2018).

3 | MATERIALS AND METHODS

Sixty-seven micromorphology blocks were collected from the six study sites in 2015 and 2016. In most cases, we sampled from the archaeological site and from test pits and stratigraphic sections located some distance from the excavation area. Off-site sampling localities were chosen to avoid anthropogenic influence and capture the natural stratigraphy as much as possible. However, at some sites (Keystone Dune and Cook) archaeological excavation walls were the only stratigraphic exposures available. In these cases, sample collection was done in areas devoid of any obvious archaeological feature or anthropogenic disturbance.

Our sampling strategy focused on previously identified buried soil horizons and sediment units (see Supporting Information Materials). Sample collection involved vertically cutting out a block of undisturbed soil or sediment with a knife and a trowel. Sample blocks were wrapped in plaster and carefully labeled to preserve their orientation and microfacies. Average plaster block size was 10 × 10 × 20 cm. In a few cases (e.g., Keystone Dune), we could not cut cohesive blocks of sediment (e.g., sandy texture), so we used smaller blue plastic electrical boxes (9.3 × 5.5 × 8.5 cm) to collect samples (Josephs & Bettis, 2003).

After collection in the field, blocks were set out to dry for one to 3 weeks before shipping. Samples were impregnated with unpromoted polyester resin (Advance Coatings, Westminster, MA) diluted with styrene in a 7:3 ratio. To catalyze the reaction, methyl ethyl ketone peroxide (MEKP) was added to the diluted resin/styrene mixture in the ratio of 7 mL–1 L of resin/styrene mixture (following Goldberg, 2000; Miller & Goldberg, 2009). After the resin mixture was added, samples were slowly air-dried over 10–12 days, and once hardened, samples were oven-dried at 60°C for 48 hr to cure the resin.

Hardened blocks were sent to Quality Thin Sections (QTS, Tucson, Arizona) and Spectrum Petrographics (Vancouver, WA) for thin section production. During thin section production, sample blocks were trimmed to 75 × 50 mm with a rock saw. Larger blocks were subdivided to provide sufficient coverage of the entire block; these samples were labeled a and b for the upper and lower portions of the blocks, respectively. Next, blocks were cut into slabs and processed into 5 × 7 cm thin sections with a standard thickness of 30 μm. Generally, thin sections were prepared vertically. However, sample blocks from Mead and Swan Point were larger in size and allowed for preparation of horizontal thin sections. A notch was cut into each thin section to indicate orientation (i.e., the notch represents "up" or "top").

Thin section analysis was completed in the micromorphology laboratory at the University of Tübingen and the petrography laboratory at the University of Arizona. Ninety-five thin sections were qualitatively described using the naked eye and a petrographic microscope. Descriptions were made under plane polarized light (PPL) and cross-polarized light (XPL), with magnifications ranging from 0.65× to 40×. Descriptive nomenclature follows Courty et al. (1989) and Stoops (2003). Photomicrographs presented in the text (Figures 4–11) and Supporting Information Materials (Figures S20–S24) are oriented so that the top of the image is topographically above the bottom of the image. For additional details on micromorphology description and photography methods, see Table 1 and the Supporting Information Materials.

Radiocarbon dates were calibrated to IntCal13 (2-sigma confidence interval) using the Calib v7.1 software program (Stuiver, Reimer, & Reimer, 2019). The Supporting Information Materials contain more information about radiocarbon sample pretreatment and laboratory analysis.

4 | RESULTS

Our analysis identifies several distinctions between our study sites in terms of microstructure, organic matter type and abundance, and the abundance and expression of pedofeatures. Additionally, micromorphology reveals the presence of different types of organic bands and stringers, particularly at the Mead and Hurricane Bluff sites. We place these organic-rich layers into different categories based on the degree of organic humification, degree of bioturbation, open versus compact microstructures and abundance of pore space, and gradual versus abrupt boundaries. The Supporting Information Materials provide more detailed results.

4.1 | Groundmass, basic mineral composition, grain size, and grain sorting

Generally, Late Glacial stratigraphic units exhibit more poorly sorted grains, while Holocene and modern units exhibit moderately to well-sorted grains. Additionally, the Late Glacial units exhibit the greater ratio of coarse grains (defined here as >0.0625 mm, predominantly sand) to fine grains (defined here as <0.0625 mm, predominantly silt in our samples; Table 2). Although subtle in thin section, fining upward is a common pattern noted throughout sand sheets, dunes, and loess blanketing the region (Dilley, 1998; Muhs et al., 2003; Potter, 2009; Reuther, 2013). In both Late Glacial and Holocene units, groundmass commonly consists of a fine-grained and coarse-grained mineral fraction, fragments of organic matter and plant residues, and iron oxide nodules. In Keystone Dune samples, the coarse fraction dominates as one would expect in a sand dune context; alternatively, in Cook samples, there is a predominant fine, condensed micromass within the loess matrices.

Late Glacial units at each site demonstrate notable features in terms of grain size variation and sorting (Table 2). At Swan Point, Late Glacial units, such as C4 and C5, contain microscale fining or
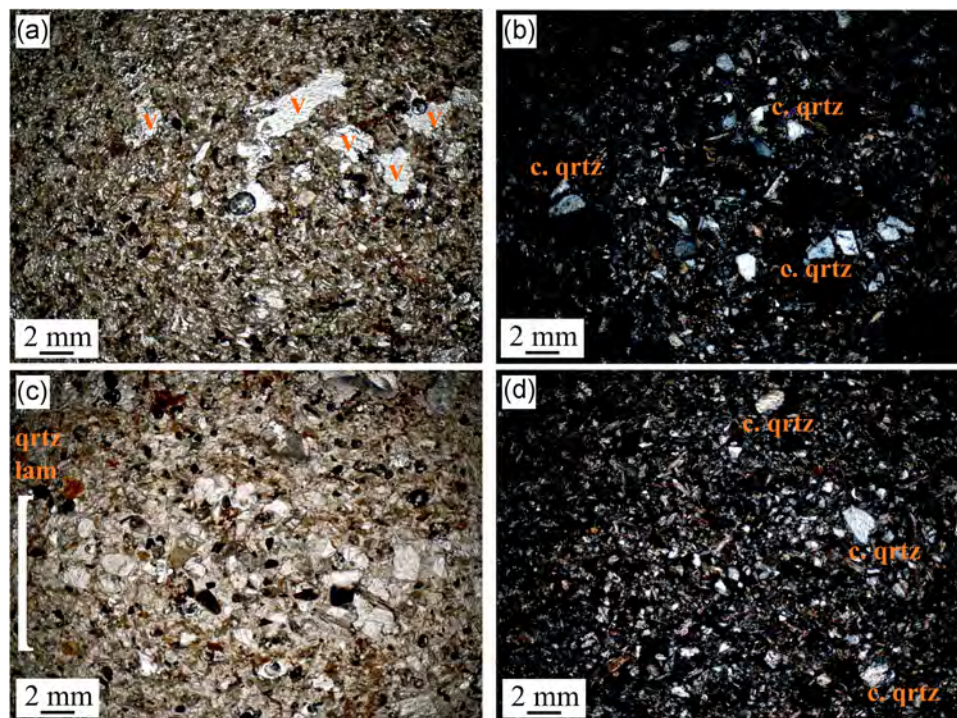
FIGURE 4 Grain size variation Swan Point samples. "C. qrtz" indicates coarse sand-sized quartz mineral grains, and "v" indicates voids. All images are at 5× magnification. (a) SP16-MM07A: Fine-grained groundmass in lower portion of thin section, lower gray sand unit, PPL. (b) SP16-MM07A: Coarse-grained groundmass in upper portion of thin section, lower gray sand unit, XPL. (c) SP16-MM13B: quartz microlamination (indicated by the white bracket), C3 horizon of soil test pit, PPL. (d) SP16-MM13A: poorly sorted groundmass in C3 horizon of soil test pit, XPL. PPL, plane polarized light; XPL, cross-polarized light [Color figure can be viewed at wileyonlinelibrary.com]

coarsening sequences and microlaminations (Figure 4a–d). Fine-grain cappings also appear in the C2 and C4 units of the test pit, which are correlated to Late Glacial units in the main excavation (Figures 5a–c, S20A, and S20B). At Mead, we observe numerous fine lenses of coarser mineral grains (quartz and muscovite) associated with organic matter fragments ("stringers"), particularly at the lower boundaries of the Upper Paleosol Complex and Lower Paleosol Complex (Figure 6a–f). We also observe fine-grain cappings in the Upper Paleosol Complex. At the Camp section, only samples from the Lower Paleosol Complex exhibit subtle grain size variations. Keystone Dune samples are well-sorted and relatively homogenous in terms of grain size. However, we observe two microlaminations in Ab2 and Ab3, associated with weakly oriented and moderately to poorly sorted quartz grains. Pedocomplexes 3, 4, and 5 also exhibit subtle coarsening or fining upward through an individual thin section. At Cook, Late Glacial stratigraphic units exhibit coarser grain sizes, moderate to poor sorting, and a few examples of vertical grain size variation.

Holocene units at Hurricane Bluff vary in grain size characteristics. Late to Middle Holocene soil units (Paleosol 9 through Pedocomplex 6) are relatively homogenous in terms of grain size and sorting, whereas Middle to Early Holocene units (Pedocomplex 5 through Pedocomplex 1) exhibit grain size variation and

bedding features. For example, Pedocomplex 5 exhibits at least four layers with different grain sizes and poor sorting. Pedocomplex 1 and the underlying units appear laminated with weak bedding development and weakly oriented quartz and muscovite grains (Figure 7).

4.2 | Microstructure and void type

Our study sites vary in microstructure and void type from the Late Glacial to Holocene (Table 3). Most Swan Point and Mead samples have vugh and/or channel microstructure. However, Late Glacial units and the Late Holocene Bw horizon at Swan Point exhibit platy and/or lenticular microstructure (Figure 5a–c). At Mead, only the Late Glacial Upper Paleosol Complex contains platy microstructure just below a thick organic band (thought to be an Ab horizon; Figures 5e,f, S20C). Pore space is abundant in samples from both sites. At Camp, Late Glacial soils appear highly bioturbated with extensive pore space (Figure 8a–d). Keystone Dune samples have massive microstructure with simple packing voids. Cook samples commonly have a condensed micromass with fewer voids. Hurricane Bluff samples vary in microstructure, although vugh and channel microstructures are common.
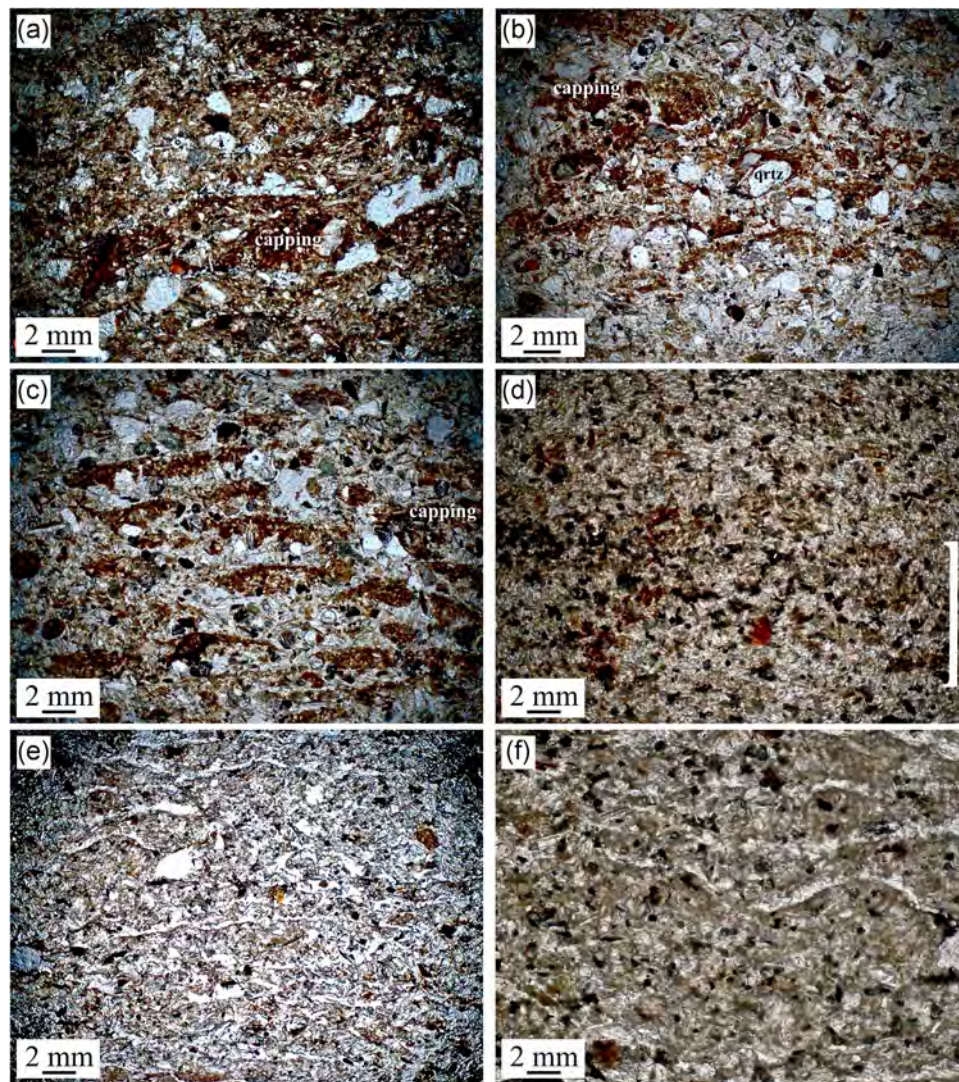
FIGURE 5 Freeze-thaw features and microstructures observed in the Swan Point and Mead test pits. All images are in PPL and 5× magnification, unless noted otherwise. (a) SP16-MM11A: Ice-lensing and fine-grain cappings in the Bw horizon. (b) SP16-MM12A: Fine-grain cappings and ice-lensing features in the C2 unit. (c) SP16-MM12A: Well-expressed ice-lensing features, fine-grain cappings, and incipient lenticular microstructure in the C2 unit. (d) SP16-MM13A: Banded concentration of humified organic matter (indicated by white bracket), C4 unit. (e) MD15-MM01B: Platy microstructure below the upper Ab horizon, Upper Paleosol Complex. (f) MD15-MM01B: Platy microstructure below the upper Ab horizon, Upper Paleosol Complex, 10× magnification. PPL, plane polarized light [Color figure can be viewed at wileyonlinelibrary.com]

4.3 | Organic matter

Organic matter is abundant at our study sites (Table 4). Organic tissue from herbaceous vegetation is most common. However, we observe increased input of "woody" organics in the Holocene-age Bwb horizons at Cook and Pedocomplexes 5 and 1 at Hurricane Bluff. At all sites, we observe abundant finely comminuted, humified organic matter, especially in layers of enriched organic matter (e.g., buried soil horizons). Modern roots and well-preserved plant fragments with visible cellular structure are also abundant, especially at the Camp section. In the Late Glacial paleosols at Camp, there is extensive mixing of organic matter with different degrees of humification (e.g., modern and humified organics; Figure 8e). Combusted organics (e.g., charcoal) are rare, observed only in the Late Holocene

Ab/Bb units at Cook and the Early Holocene Pedocomplex 1 at Hurricane Bluff. Organic matter is most abundant in Hurricane Bluff samples, especially from the Early Holocene (Figure 7b, 7e). Bands and thinner stringers of concentrated organic matter are also common at Hurricane Bluff.

4.4 | Pedofeatures

Our study sites show significant variation in the abundance and type of pedofeatures (Table 5). The Mead site contains the greatest number of pedofeatures (Figure S21). Swan Point, Camp, Keystone Dune, and Cook have fewer pedofeatures, but they do contain bioturbation and passage features (i.e., animal and/or insect
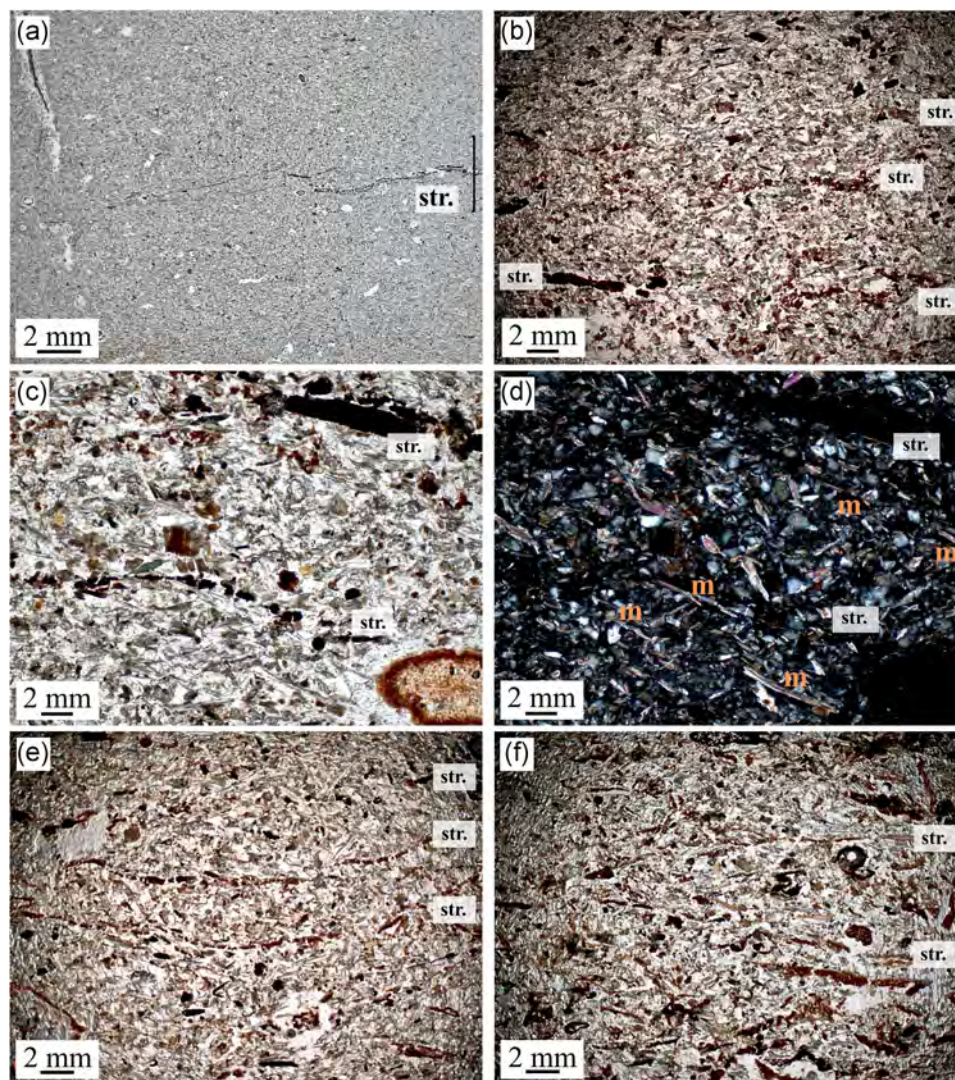
FIGURE 6 Very thin (mm scale) organic stringers (labeled "str") associated with weakly oriented muscovite grains (labeled "m") at the Mead site. Images (a)–(d) are from the Upper Paleosol Complex, and images (e)–(f) are from the Lower Paleosol Complex. Images are all in PPL, except for image (d) (XPL). (a) MD15-MM02B, 0.65×. (b) MD15-MM02B, 5×. (c) MD15-MM02B, 10×. (d) MD15-MM02B, same as (c), XPL. (e) MD15-MM04A, LPC, 5×. (f) MD15-MM04B, 5×. PPL, plane polarized light; XPL, cross-polarized light [Color figure can be viewed at wileyonlinelibrary.com]

burrows). Hurricane Bluff appears intermediate in terms of pedofeature abundance and shares some similarities with Mead.

The main pedofeatures at Swan Point are bioturbation from root growth (particularly in the Late Holocene units), iron oxide impregnation of the matrix, and iron oxide mottling and horizontal banding in the Late Glacial units (especially at the test pit location). At Mead, both Late Glacial pedocomplexes contain bands of concentrated, humified organic matter (Figures 9, S21A, and S21C), iron oxide hypocoatings (Figures 10 and S22), and micritic calcite hypocoatings (Figures 10, 11, and S23). In each case, iron oxide hypocoatings superimpose the micritic calcite hypocoatings (Figures 10 and S22). We also see a layer of sparitic calcite between the Lower and Upper Paleosol Complexes (Figures 11c,d and S21D), well-developed iron-oxide quasi-coatings in the Upper Paleosol Complex (Figure S21B), and iron oxide mottling above the Upper Paleosol Complex.

Camp samples exhibit few, weakly expressed pedofeatures. In the Late Glacial Lower Paleosol Complex, we see few calcite hypocoatings, coatings, and calcified roots. In the Middle and Lower Paleosol Complexes, there are two passage features and extensive root bioturbation (Figure 8f). Similarly, Late Glacial samples from Keystone Dune contain few pedofeatures. In Pedocomplex 3 and the associated Ab horizon, we observe weak iron oxide staining of the matrix associated with thin concentrations of organic matter. In Pedocomplex 4, Ab4, and Pedocomplex 5, there is localized iron oxide staining around root pores and moderate impregnation of the matrix. At Cook, the most common pedofeature is iron oxide impregnation of the matrix, especially in Holocene units. Most Late Glacial samples contain few weakly expressed pedofeatures or appear nonpedogenic. At Hurricane Bluff, Early Holocene stratigraphic units contain more pedofeatures than the Middle or Late Holocene units. The most common pedofeatures are
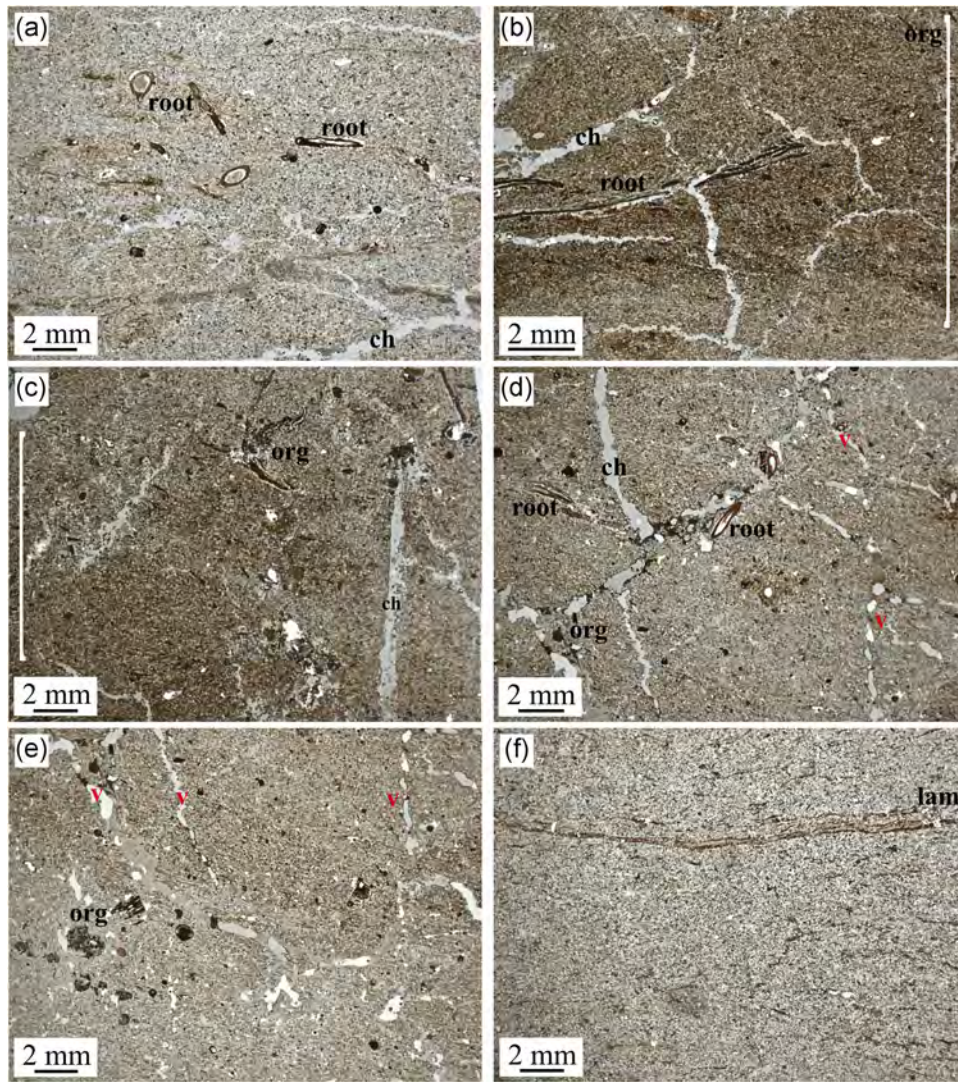
FIGURE 7 Organic matter laminations and pedofeatures present in Pedocomplex 1 at the Hurricane Bluff site. In each image, examples of root fragments are labeled as "root," organic fragments are labeled as "org," lamination features are labeled as "lam," channel voids are labeled as "ch," and interconnected voids are labeled as "v." White brackets point out areas of concentrated organic matter, humification, and iron oxidation (indicative of pedogenesis). All images are in PPL. (a) HB15-MM09: Very thin (<2 mm) laminations and larger organic/root fragments, 0.65×. (b) HB15-MM10 (bottom): Thicker (cm scale) band of concentrated organic matter and iron oxidation with channel microstructure, 0.65×. (c) HB15-MM10 (top): Thicker band of concentrated organic matter and iron oxidation, 0.65×. (d) HB15-MM11 (top): Fragmented organic matter, roots, and very thin laminations with channel and spongy microstructure, 0.65×. (e) HB15-MM11 (middle): Organic matter fragments, interconnected vughs (spongy microstructure), and groundmass with laminated appearance, 0.65×. (f) HB15-MM13 (bottom): Very thin, organic laminations and groundmass with a laminated appearance, 0.65×. PPL, plane polarized light; XPL, cross-polarized light [Color figure can be viewed at wileyonlinelibrary.com]

heavy bioturbation, iron oxide hypocoatings, and iron oxide impregnation in linear bands. Calcite features are also present in Pedocomplex 1 and the underlying stratigraphic units (Early Holocene). We should note that some samples from the same units contain few pedofeatures, suggesting lateral variability across the bluff exposure.

Finally, all of our study sites contain concentrations of organic matter, which vary in terms of thickness, microstructure, bioturbation, humification, and boundary characteristics. At Mead and Hurricane Bluff, we observe two types of organic-rich layers:

(a) thicker (cm scale) bands with greater bioturbation and humification, open microstructure, and gradual boundaries, and (b) thinner (mm scale) stringers with abrupt boundaries, little to no mixing into the groundmass, and association with oriented mineral grains (Figure S24). The thinnest stringers are not visible in the field but have been incorporated into thicker pedocomplexes, particularly toward the lower boundaries. In Swan Point, Camp, Keystone Dune, and Cook samples, organic-rich bands tend to be thicker (cm scale) and weakly bioturbated; they also lack a laminated appearance and/or thin (mm scale), abrupt stringers associated with oriented mineral grains.
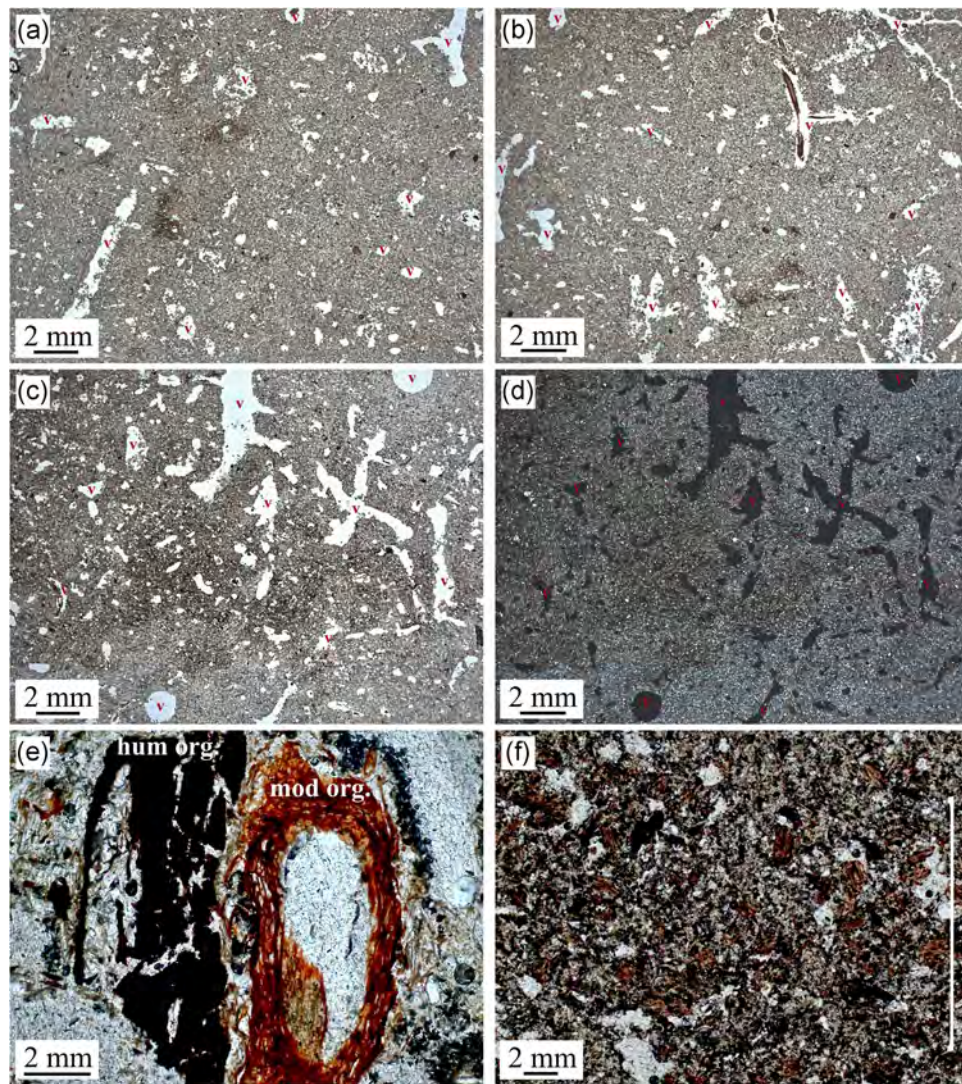
FIGURE 8 Open microstructure, heavy organic bioturbation, and mixing of organic matter within the Middle Paleosol Complex (images a, b, and f) and Lower Paleosol Complex (images c, d, and e) at the Camp section. In each image, voids are labeled "v." In panel (e), humified organic matter is labeled as "hum org," and modern organic matter is labeled as "mod org." All images are in PPL and 0.65× magnification, unless noted otherwise. (a) Sample CP16-MM01B. (b) Sample CP16-MM01B. (c) CP16-MM02A. (d) Same sample as C (CP16-MM02A), image in XPL. (e) Sample CP16-MM01A: Organic root fragments exhibiting different degrees of humification (humified on the left, modern with preserved cellular structure on the right) immediately adjacent to one another within the Middle Paleosol Complex, 5×. (f) Sample CP16-MM01A: A passage feature of mixed, disturbed organic matter (white bracket) in the Middle Paleosol Complex, indicative of animal burrowing, PPL, 5×. PPL, plane polarized light; XPL, cross-polarized light [Color figure can be viewed at wileyonlinelibrary.com]

5 | DISCUSSION

Our study addresses several research questions regarding the unique subarctic soils and sediments present in our stratigraphic sections. Using micromorphology, we test the field interpretation that dark brown stringers, found across SCF and commonly dated to the Late Glacial, are buried soils. These stratigraphic units appear broadly similar from site to site and therefore are interpreted to be the result of the same process (i.e., pedogenesis); however, our microscale analysis demonstrates that other processes (e.g., deposition, localized reworking of organic matter, solifluction) likely contributed to their formation. In this way, micromorphology serves as a valuable technique for addressing issues of

equifinality when interpreting subarctic stratigraphy and helps revise interpretations of what constitutes a true soil horizon in our study region. In turn, this has implications for accurately reconstructing the paleoenvironment and landscape inhabited by early human colonizers of the area. Micromorphology also reveals evidence of bioturbation and cryoturbation not previously recognized at our sites. Although the degree of mixing is not significant enough to alter artifact provenience, this disturbance could impact certain paleoenvironmental proxies, such as pollen assemblages, ancient DNA, and organic geochemical proxies.

Additionally, our analysis provides a useful test for the idea that these study sites are broadly similar in terms of site formation history, pedogenesis, and sedimentology, and by extension, each site serves as a
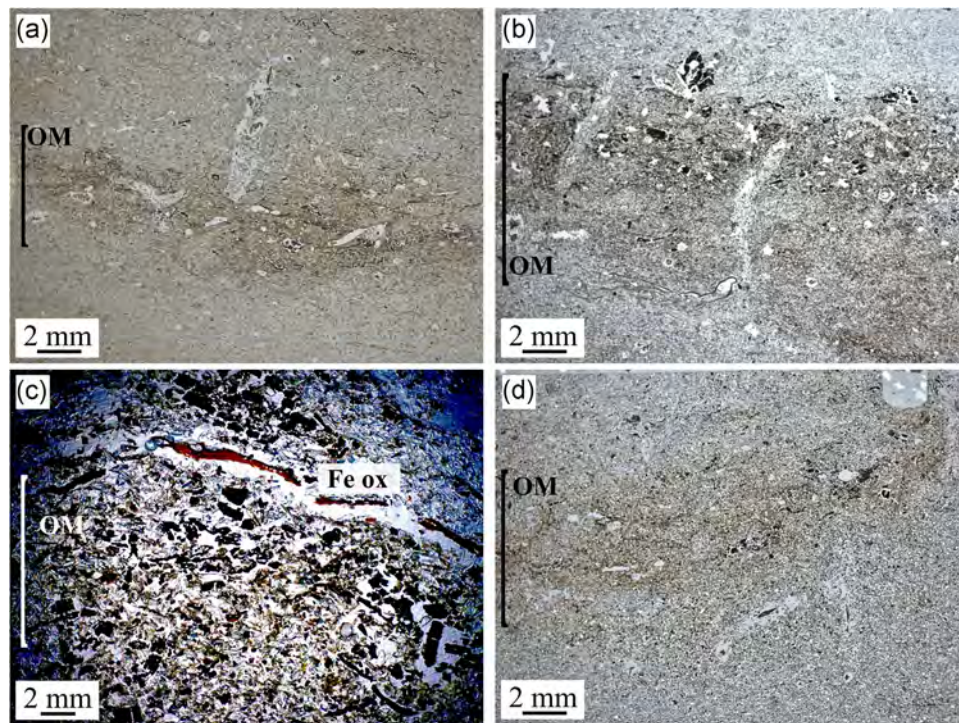
FIGURE 9 Examples of thicker, pedogenic bands enriched in OM, Upper Paleosol Complex, Mead site soil test pit. All images are in PPL. (a) MD15-MM01B: Organic enrichment and iron oxidation in the lower Ab horizon, 0.65×. (b) MD15-MM01B: Organic matter humification and enrichment in upper Ab horizon, 0.65×. (c) MD15-MM01B: Humified organic matter and linear bands of iron oxidation within the upper Ab horizon, 5×. (d) MD15-MM02B: Humified organic matter in upper Ab horizon, 0.65×. OM, organic matter; PPL, plane polarized light [Color figure can be viewed at wileyonlinelibrary.com]

stand-alone archive for regional environmental and climatic conditions. Our results disprove this hypothesis and demonstrate unexpected microscale variation from site to site, supporting recent work that emphasizes the importance of landscape heterogeneity for site formation and paleoecology (Lanoë, Reuther, Holmes, & Potter, 2020; Reuther, 2013). We observe significant intersite differences in vertical grain size variation, degree, and expression of pedogenesis, carbonate precipitation, iron oxidation and redoximorphic features, types and mixing of organic matter, and the extent of freeze-thaw activity, indicating that local and/or microenvironmental conditions at each study locality were the dominant controls on site formation (Table 6). Therefore, researchers must exercise caution when interpreting individual sites in terms of regional or global processes. Many of these findings are unobservable in the field, demonstrating the power of micromorphology to improve models of site formation and paleoenvironmental reconstruction in the subarctic.

5.1 | Do Late Glacial stringers represent buried soils, or do they instead represent processes other than pedogenesis? Which mechanisms explain the nonpedogenic stringers?

Previous studies describe stringers as paleosols based on their dark brown color, organic enrichment, evidence of bioturbation, and relative continuity across site landforms (Dilley, 1998; Potter et al., 2007; Reuther et al., 2018). However, we find that not *all* dark brown, organic-rich layers

at these sites are true buried soils. Instead, the answer to this question varies by site; most sites show weak or no pedogenesis associated with thin stringers of the Late Glacial, whereas the Mead site exhibits more extensive pedogenesis. At Mead, we support the interpretation of thicker, organic-rich bands (3—5 cm) as buried soils, based on diffuse boundaries, bioturbation, and humification of organic matter (Figures 9, S21A, and S21C). By contrast, the thinnest organic stringers (often <1 cm thick) appear depositional based on the lack of bioturbated organic matter, the presence of sharp, abrupt boundaries, and the association with weakly oriented muscovite grains (Figures 6, S21E, and S21F). Deposition is also indicated by the abrupt, angular, lower boundary of the Late Glacial Lower Paleosol Complex and abundant thin stringers in the lower portions of each Late Glacial pedocomplex. Microdepositional features indicate a less stable and more dynamic landscape than implied by soil formation alone.

Processes related to periglacial environments (i.e., areas adjacent to glaciers or ice sheets) could explain the presence of these nonpedogenic stringers. Seasonal sheet wash events and/or solifluction, especially during spring thaw, are potential mechanisms for mobilizing organic material (e.g., patchy vegetation) and fostering an active surface (Thorson, 1990). Heightened landscape instability in the spring and early summer may have washed organic matter into areas of lower topography, which was then followed by soil formation. As sheet wash and/or solifluction processes decreased and the slope stabilized, soil formation may have intensified (indicated by the thicker bands of organic matter higher in each pedocomplex).
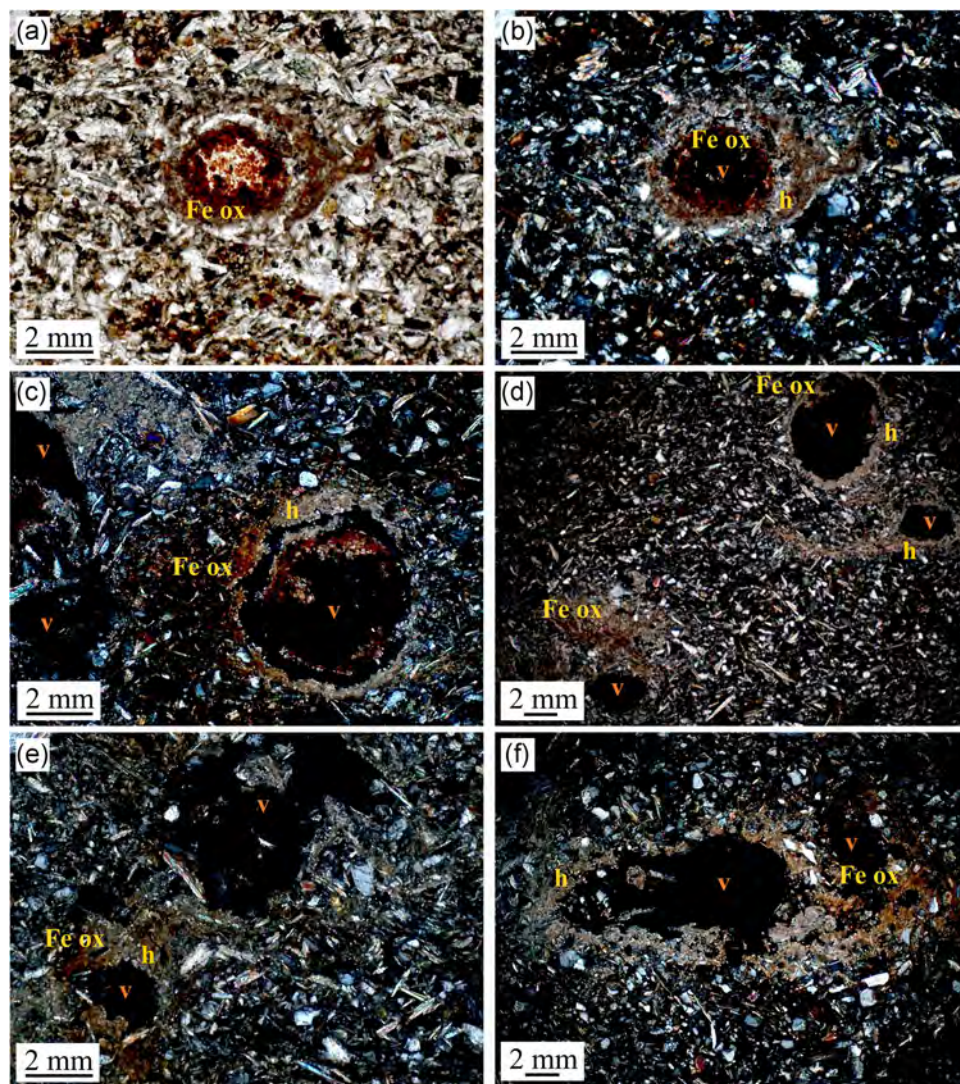
FIGURE 10 Examples of iron oxides superimposed on calcite pedofeatures within and between the Upper and Lower Paleosol Complexes at the Mead site. Iron oxides are labeled as "Fe ox," calcite hypocoatings are labeled as "h," and voids are labeled as "v." Only Image (a) is in PPL; other images are in XPL. (a) MD15-MM01B, Upper Paleosol Complex, 10×. (b) MD15-MM01B, Upper Paleosol Complex, 10×. (c) MD15-MM02A, Upper Paleosol Complex, 10×. (d) MD15-MM03A, between Lower Paleosol Complex and Upper Paleosol Complex, 5×. (e) MD15-MM04A, Lower Paleosol Complex, 10×. (f) MD15-MM05A, bottom Lower Paleosol Complex, 5×. PPL, plane polarized light; XPL, cross-polarized light [Color figure can be viewed at wileyonlinelibrary.com]

Over time, organic stringers could have been incorporated into the pedocomplex, eventually becoming indistinguishable from true soil horizons in the field. This provides a useful example of local-scale landscape heterogeneity, common along sloping bluff or terrace landforms (e.g., Thorson & Tryon, 2003); one portion of the landform can experience instability, while other portions are more stable.

At Swan Point, previous studies describe thin paleosols associated with early archaeological occupations in the Late Glacial lower silt and sand units (Dilley, 1998; Holmes, 2001). However, if soils formed at Swan Point during this period, we would expect to see bands of humified, bioturbated organic matter in thin section. Instead, we observe little evidence of pedogenesis. Researchers have noted that ground freezing can produce "pseudo-stratification" and "pseudo-paleosols" in subarctic loamy sediments, like those present

at Swan Point (Thorson, 1990). If the sediment is moist, various components of the substrate (such as organic matter, humic colloids, dissolved ions, and fine mineral grains) can be preferentially concentrated at the freezing point (Thorson, 1990, p. 406). Over time, this process results in the formation of "organically stained subparallel bands" of fine-grain particles that trap downward-moving components (Schuman & Rieger, 2007, p. 29; Thorson, 1990, p. 406). Such bands can easily be mistaken for very weakly developed A or B horizons. This may be the case in the Swan Point excavation area, where Dilley (1998) originally defined these Ab horizons. Addition of anthropogenic materials, such as hearth charcoal and organics, further complicates interpretation of these "pseudo soils." We suspect that freeze-thaw processes concentrated material in subparallel bands, giving the illusion of Late Glacial soil formation at this site.
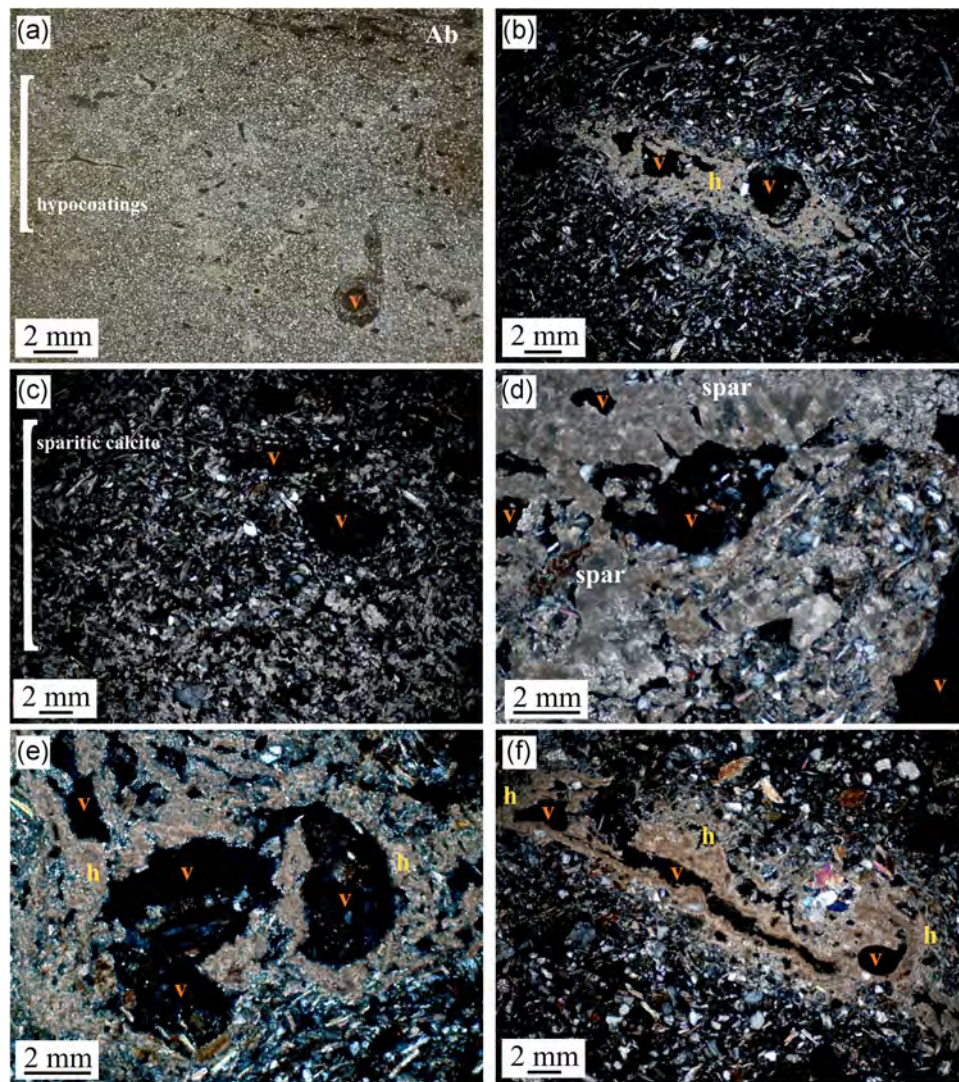
FIGURE 11   Micritic calcite pedofeatures (a,b) in the Upper Paleosol Complex (a,b) and Lower Paleosol Complex (e,f), compared to sparitic calcite between the Upper Paleosol Complex and Lower Paleosol Complex (c,d), Mead site soil test pit. In each image, calcite hypocoatings are labeled as "h," voids are labeled as "v," and sparitic calcite is designated as "spar." All images are in XPL. (a) MD15-MM01B: Zone of concentrated micritic calcite hypocoatings (mini Bkb horizon), 0.65×. (b) MD15-MM02A: Well-developed micritic calcite hypocoating, 5×. (c) MD15-MM03A: Layer of sparitic calcite with visible calcite rhombs, 5×. (d) MD15-MM03A: Detailed view of sparitic calcite, 10×. (e) MD15-MM04A: Well-developed calcite hypocoatings and calcite impregnation of the matrix around voids, 10×. (f) MD15-MM04B: Well-developed calcite hypocoating around an elongated root void, 5× [Color figure can be viewed at wileyonlinelibrary.com]

Based on our analysis, "stringers" in the lower units at Swan Point (Figure 5d) are not true buried soils, which implies a more dynamic and instable Late Glacial landscape than previously recognized.

At Keystone Dune, previous descriptions note a series of at least 16 buried Entisols (Ab horizons) within the Late Glacial sequence (Reuther, 2013; Reuther et al., 2016). In the field, these soil horizons are very thin (0.5–2 cm), dark brown or black in color, and contain numerous charcoal fragments (Reuther, 2013; Reuther et al., 2016). In thin section, most of these organic lenses have a bioturbated, humified appearance, supporting a pedogenic interpretation. However, there is variability in the abundance and distribution of pedogenic features and charred plant fragments across the Keystone Dune section, as discussed in Section 5.4.

Our study indicates weak or no pedogenesis at Camp and Cook during the Late Glacial. At Camp, the two thicker, organic-rich bands are correlated to the Middle and Lower Paleosol Complexes at Broken Mammoth, and secondary calcite has been used as the primary diagnostic feature of pedogenesis (Dilley, 1998). In our analysis, Lower Paleosol Complex samples exhibit calcite hypocoatings and calcified roots in low abundance, while Middle Paleosol Complex samples exhibit only bioturbation and few pedofeatures. The limited abundance of pedofeatures indicates weak pedogenesis at this site. At Cook, evidence of pedogenesis is even weaker. Late Glacial stringers are enriched in organic matter, but they contain few diagnostic pedofeatures. Stringers in the upper stratigraphic sequence also exhibit few pedofeatures. One possibility is that stringers at

TABLE 1 Explanation of micromorphology description categories used in this study

Feature	Definition	Utility in this study
Groundmass	General term for base material of soil in thin section; includes coarse and fine material and packing voids, excludes pedofeatures	Nature of source material and spatial relationship between soil units
Composition	Lithology and/or material that makes up the sample	Nature of parent material or degree of alteration
Grain size and sorting	Size of mineral grains within the sample and how evenly distributed certain grain sizes are	Energy of deposition, association between grain sizes and sedimentological processes
Microstructure	Relationship between solid constituents and voids (aggregated and nonaggregated material)	Characteristic of particular soil types, can reflect internal or external oriented pressures
Voids	Spaces not occupied by solid soil material	Disturbance processes, soil ped formation and distribution
Organic matter type and abundance	Organic matter present in the sample and relative concentration/quantity	Vegetation types on the past landscape, degree of soil formation, and postdepositional disturbance (bioturbation)
Pedofeatures	Discrete fabric units present in soil materials, distinguished from an adjacent material by a difference in concentration or internal fabric	In situ vs. inherited features, relative timing of pedogenic processes, changes in climate or geomorphology that influenced soil formation

Note: Definitions and terms from Stoops (2003) and Stoops et al. (2010).

Cook represent faint accumulations of herbaceous vegetation over short time scales (e.g., a few years to 10 s of years). Additional micromorphological analysis (i.e., horizontally and vertically across a section) should be conducted to confirm or reject classification of the Cook stringers as buried soils.

Although Holocene in age, Hurricane Bluff is similar to Mead in terms of exhibiting both pedogenic and nonpedogenic stringers. Our micromorphology analysis supports a pedogenic interpretation for the upper paleosols (Paleosols 7–10), as they have a bioturbated and humified appearance typical of buried soils. We also find pedogenic characteristics in thicker, organic-rich bands within the Middle to Early Holocene soil units (Pedocomplexes 6, 2, and 1; Figure 7b,c). However, micromorphology reveals the presence of thinner, non-pedogenic, laminated organic layers and fine-scale bedding sequences (mm-to-cm scale) in the lower portion of these units (Figures 7a, 7d–f, and S24). These thin stringers may reflect similar processes that occurred in the Late Glacial (at Mead) and again in the Holocene (at Hurricane Bluff). Both sites are close to river confluences with braided beds, which provide abundant sediment for aeolian transport. Aeolian deposition may have been high enough to maintain early successional cycles of vegetation and restrict the growth of thicker moss beds or forest litter that would foster more developed soils. Alternatively, these stringers could be the result of localized reworking of organic matter through mechanisms common in periglacial environments (e.g., permafrost formation, seasonal melt), based on depositional characteristics and association with oriented mineral grains (Thorson, 1990).

In regard to our first research question, micromorphology proves to be a valuable tool for addressing issues of macroscale equifinality. In the field, stratigraphic variability from site to site is notable (Figure 3), but Late Glacial "stringers" still bear a superficial resemblance (Figure 1). At the microscale, these stringers exhibit striking differences. We observe that stringers likely resulted from dramatically different processes and interactions between soil formation, freeze-thaw activity, and/or aeolian deposition at each site.

5.2 | Which pedogenic processes are associated with buried soils and paleosol complexes at the study sites? What can buried soils tell us about local landscape conditions?

Based on our analysis, Mead experienced the most extensive Late Glacial soil development of our six study sites. Therefore, our discussion of pedogenic processes focuses on the Mead site. Abundant calcite and redoximorphic pedofeatures shed light on mechanisms of soil formation and local environmental and hydrologic conditions. To trace broader environmental shifts at the site, we thoroughly examined thin sections to determine the stratigraphic relationship between these pedofeatures, that is do we observe alternating precipitation of secondary calcite and iron, or conversely, does one pedofeature always superimposes the other? The presence of these two pedofeatures and their relationships help elucidate periods of moisture versus aridity, and periods of free drainage versus water saturation.

In the Lower Paleosol Complex, redoximorphic features consistently superimpose calcite pedofeatures, so we propose that calcite hypocoatings formed first and redoximorphic features formed at a later point in time (Figures 10 and S22). Micritic calcite pedofeatures tend to form in the vadose zone (above the water table), where sporadic wetting fosters the growth of smaller crystals (Miller & Goldberg, 2009; Stoops, Marcelino, & Mees, 2010). Micritic hypocoatings in the Lower Paleosol Complex suggest a well-drained landscape during soil formation. These hypocoatings likely formed due to downward percolation of soil solutions through root voids,

TABLE 2 Summary of descriptions of groundmass, composition, grain size and grain sorting at all study sites

Site	Strat unit	Groundmass/lithology	Grain size	Sorting	Textural features	Examples
Swan Point—main exc.	A/Bw/C	Mineral grains (qrtz/musc), iron oxides, organics	Silt/f.s.	Well-sorted to moderate	Very fine groundmass, tightly packed grains	SP16-MM04
	Gray silt	As above	Silt/m.s.	Moderate to poor	Greater c/f ratio	SP16-MM06A
	Gray sandy silty	As above	M.s./c.s.	Moderate to poor	Vertical and lateral variability in grain sorting; Greater c/f ratio	Figure 4
—test pit	A/Bw/C	As above	Silt	Moderate	Fine groundmass	SP16-MM11A/B
	C1	As above	Silt/f.s.	Moderate	Fine-grain cappings; translocation of fines	Figure 5
	C3	As above	Silt/m.s./c.s.	Moderate to poor	Microlaminations; Greater c/f ratio	SP16-MM13A/B
Mead	Upper mottled sediment	Mineral grains (qrtz/musc), Fe ox	Silt	Well-sorted	–	MD15-MM08
	Upper Paleosol Complex	Mineral grains (qrtz/musc), Fe ox, carbonates, OM	Silt/f.s.	Moderate	Thin organic stringers; fine-grain cappings	MD15-MM01-MM02; Figure 6
	Lower Paleosol Complex	As above	Silt/f.s.	Moderate	Thin organic stringers	MD15-MM04-MM05; Figure 6
Camp	Middle Paleosol Complex	Mineral grains (qrtz/musc), Fe ox, OM	Silt/m.s.	Well to moderate	No vertical variation in grain size	CP16-MM01
	Lower Paleosol Complex	As above, with carbonates	Silt/m.s.	Well to moderate	Subtle grain size variations; thin lenses of c.s.	CP16-MM03A/B
KDS	Late Glacial sequence (Ab2 –Pedo #5)	Mineral sand grains (qrtz), Fe ox, OM	F.s./m.s.	Well-sorted	Microlaminations in Ab2, Ab3, Ab4; vertical grain size variations in Pedo #3-#5	KDS15-MM14/ MM15/MM21
Cook	Ab/Bb/C	Mineral grains (musc/qrtz), Fe ox, OM	Silt/f.s.	Well to moderate	Coarser and fine fractions present	CK15-MM10
	Bwb2/Bwb5/C6	As above	Clay to silt	Well-sorted	Very fine, condensed micromass	CK15-MM11/MM12
	Late Glacial units	As above, with carbonates	F.s./m.s./c.s.	Moderate to poor	Some samples with vertical variation in grain size	CK15-MM02
Hurricane Bluff	Paleosol 9-Paleosol 7	Mineral grains (qrtz/musc), Fe ox, OM	Silt to f.s.	Moderate	More homogeneous grain size/sorting	HB15-MM01-MM03B
	Pedocomplex 6-Paleosol 1	As above	Silt to f.s.	Moderate	Bedding features/microlaminations (P5, P1)	HB15-MM04B; Figure 7

Note: Dominant lithology is always listed first.

Abbreviations: c/f ratio, ratio of coarse to fine grains; c.s., coarse sand; Fe ox, iron oxides; f.s., fine sand; m.s., medium sand; musc, muscovite grains; OM, organic matter; P, Paleosol; qrtz, quartz grains.

TABLE 3 Summary of descriptions of microstructure and void type(s) all study sites

Site	Strat unit	Microstructure(s)	Void type(s)	Notes	Examples
Swan Point—main exc.	A/Bw/C	Vugh/spongy (Bw)/lenticular/platy (Bw-C)	Vughs, channels	Bioturbated, significant pore space	SP16-MM03B
	Gray silt	Vugh/vughy-channel to massive	Vughs, channels	Most samples bioturbated; one example of animal burrowing	SP16-MM05B
	Gray sandy silty	Vugh/vughy-channel to massive	As above	Most samples bioturbated, some contain zones of massive/condensed micromass	SP16-MM09B
—test pit	A/Bw/C	Lenticular (Bw)	Vughs, channels	Open microstructure	SP16-MM11
	C1	Lenticular	As above	Incipient to well-developed microstructure	Figure 5
	C3	Lenticular	As above	As above	Figure 5
Mead	Upper mottled sediment	Massive	Simple packing voids	Few voids	MD15-MM08
	Upper Paleosol Complex	Vugh/channel; platy below Ab	Vughs, channels, simple packing	Abundant voids	MD15-MM01-MM02; Figure 5
	Lower Paleosol Complex	Massive/channel	Channels, vughs, simple packing	Channels primarily in organic bands	MD15-MM04-MM05; Figure 5
Camp	Middle Paleosol Complex	Channel	Channels, vughs	Abundant voids and pore space	CK16-MM01A/B; Figure 8
	Lower Paleosol Complex	Channel	Channels, remnant planar voids	Abundant root channels and pore space	CP16-MM02B; Figure 8
Keystone Dune	Late Glacial sequence (Ab2 −Pedo #5)	Massive	Simple packing, channels	Packing voids = 70–80% of void space	KDS15-MM15-MM21
Cook	Ab/Bb/C	Vugh	Vughs, channels, simple packing; remnant planar voids	Abundant pore space	CK15-MM09-MM10
	Bwb2/Bwb5/C6	Channel/sbk (C6)	Remnant planar voids (Bwb5)	Weak pedality (C6)	CK15-MM11
	Late Glacial units	Channel/weak sbk	Channels, vughs	–	CK15-MM01-MM08
Hurricane Bluff	Paleosol 9–Paleosol 7	Vugh	Vughs, channels	–	HB15-MM01-MM03B
	Pedocomplex 6–Paleosol 1	Channel/spongy to vugh (P1)/lenticular to massive (below P1)	Channels, vughs	Less pore space in lower units	HB15-MM04-MM11

Note: Dominant characteristic is always listed first.
Abbreviations: sbk, subangular blocky; tp, test pit.

TABLE 4 Summary of predominant organic matter type(s) and organic matter abundance at all study sites

Site	Strat unit	Abundance	Type(s)	Humification	Features/notes	Examples
Swan Point—main exc.	A/Bw/C	Moderate (A/Bw) to low (lower C)	Root and tissue frags.	Low to moderate	–	SP16-MM01A/B
	Gray silt	Low	Root and tissue frags.	Moderate to high	–	SP16-MM05A/B
	Gray sandy silty	Moderate	Finely comminuted, root frags.	Moderate to high	Decrease in OM relative to upper units	SP16-MM07A/B
—test pit	A/Bw/C	Moderate	Root and tissue frags.	Moderate to high	–	SP16-MM11A/B
	C1	Moderate	Root and tissue frags., finely comminuted	Moderate to high	–	SP16-MM12A/B
	C3	Moderate	Root and tissue frags., finely comminuted	Moderate to high	Thin stringer (2–5 mm) present toward base of this unit	SP16-MM13A/B
Mead	Upper mottled sediment	Low	Finely comminuted	Low	–	MD15-MM08
	Upper Paleosol Complex	High	Finely comminuted, root/tissue frags.	High	Concentrated bands (10–20 mm), stringers (2–5 mm)	Figure 6
	Lower Paleosol Complex	High	As above	High	3 concentrated bands (10–30 mm), stringers (2–5 mm)	Figure 6
Camp	Middle Paleosol Complex	Very high	Root/tissue frags, finely comminuted	Moderate to high	Heavy root bioturbation, mixing of modern + humified	Figure 8
	Lower Paleosol Complex	Very high	As above	Moderate to high	Extensive mixing of modern + humified OM	Figure 8
Keystone Dune	Late Glacial (Ab2 – Pedo #5)	Moderate to high	Finely comminuted, root/tissue frags.	Moderate to high	No charcoal present; Pedo #3 = 4+ linear, organic bands	KDS15-MM15-MM21
Cook	Ab/Bb/C	Moderate to high	Finely comminuted, root/tissue frags.	Moderate to high	Microcharcoal (?) (Ab/Bb); Increased "woody" OM	CK15-MM09-MM10
	Bwb2/Bwb5/C6	Moderate	As above	Moderate	–	CK15-MM11
	Late Glacial units	Low to moderate	As above	Moderate	–	CK15-MM01-MM08
Hurricane Bluff	Paleosol 9–Paleosol 7	Very high to high	Finely comminuted, root/tissue frags.	Moderate to high	Herbaceous types dominant	HB15-MM01-MM03B
	Pedocomplex 6–Paleosol 1	Very high to high	As above	Moderate to high	Modern + humified mixing; thicker bands + stringers; "woody" OM (P5, P1); charcoal (?) (P1)	HB15-MM04A/MM05/MM11

Note: We use the following scale for abundance: low, moderate, high, and very high. Dominant characteristic is always listed first.
Abbreviations: frags., fragments; OM, organic matter.

TABLE 5 Summary of pedofeatures at all study sites

Site	Strat unit	Abundance	Calcite pedofeatures?	Iron oxide pedofeatures?	Pedogenic appearance?	Notes/features	Examples
Swan Point—main exc.	A/Bw/C	Low	None observed	Matrix impreg., weak quasi-coating (Bw)	Yes, modern (A/Bw)	bioturbation + passage features (lower C)	SP16-MM01B
	Gray silt	Low	None observed	Weak matrix impregnation	No	Passage features w/crescentic fabric	SP16-MM05B/MM06A
	Gray sandy silty	Low	None observed	As above	No	-	
—test pit	A/Bw/C	Low	None observed	Matrix impreg.	Yes (A/Bw)	Welding (Bw/C)	
	C1	Low	None observed	Mottling, banding	No	-	
	C3	Low	None observed	Mottling, lenticular banding	No	-	
Mead	Upper mottled	Low	None observed	Quasi-coatings	No	Assoc. w/voids	MD15-MM08
	Upper Paleosol Complex	High	mc hypo	W.d. quasi-coatings, hypocoatings	Yes for thicker organic bands	Hypo. layer (below Ab); Fe oxides over mc hypo	MD15-MM02A
	Between Upper & Lower Paleosol Complex	Low	spar layer	None	No	-	MD15-MM03A, Figure 11
	Lower Paleosol Complex	High	mc hypo., coatings	Quasi-coatings/hypo. assoc. w/voids	Yes for thicker organic bands	Fe oxide hypo. over mc hypo.	MD15-MM04A
Camp	Middle Paleosol Complex	Low	None	Matrix impreg./localized staining	Weak	bioturbation + passage features	Figure 8
	Lower Paleosol Complex	Moderate	mc hypo, calcified roots	Localized staining	Weak to moderate	Extensive bioturbation	Figure 8
Keystone Dune	Late Glacial (Ab2 – Pedo #5)	Low	None observed0	Weak to moderate matrix staining	Moderate	Organic bands assoc. w/Fe oxide staining	KDS15-MM16-MM21
Cook	Ab/Bb/C	Low	None observed	Weak matrix impreg.	Yes, modern (Ab/Bb)	-	
	Bwb2/Bwb5/C6	Low	Calcified plant tissue	Staining/matrix impreg.	Weak	-	CK15-MM13
	Late Glacial units	Low to moderate	mc hypo. (voids) calcified roots	Mottles and/or lenticular bands	Weak	-	CK15-MM02/MM06
Hurricane Bluff	Paleosol 9-Paleosol 7	Few to moderate	Radial carbonate forms	Matrix staining/impregnation	Yes	-	
	Pedocomplex 6-Paleosol 1	Moderate to high	mc nodules/infillings (P1)	Matrix impreg.	Varies by unit	Crescentic passage feature + burrowing (P5)	HB15-MM05B/MM06A

Note: Dominant characteristic is always listed first.

Abbreviations: hypo., hypocoatings; impreg., impregnation; mc, micritic calcite; spar, sparitic calcite; w.d., well-developed.

TABLE 6 Summary of archaeological components, macroscale stratigraphy (in-field), and microscale stratigraphic features (from our micromorphology analysis and mentioned in the main text) at our six study sites

Time period (cal yr BP)	Scales of observation	Swan point	Mead	Camp	Keystone dune	Cook	Hurricane bluff
Late Holocene (1,000–present)	Archaeological component(s)	n/a	n/a	n/a	n/a	n/a	n/a
	In-field pedostratigraphy	Modern O/E/A	Modern OA/B	Modern A/E	Modern O/A/E	Modern O, AB	P10, P9
	Micromorphology	-	-	-	-	-	Soil formation (bioturbation, humification)
Middle Holocene (6,000–1,000)	Archaeological component(s)	CZ1a, CZ1b	CZ1a, CZ1b	n/a; Broken Mammoth - CZ1a	n/a	n/a	Cultural Components 2 and 1
	In-field pedostratigraphy	Bw, BC	B, Bwb, BC	Bw, BC	B	Upper "forest soils"; C1, Bwb1, Ab/Bb, C2/Bwb2, C3/Bwb3	P8, P7, T2, PC6, PC5, P4, P3
	Micromorphology	weak ice-lensing (platy + lenticular microstructures) in lower Bw	-	-	-	Increased input of "woody" organic matter	Increased input of "woody" organic matter (PC5); soil formation (bioturbation, humification); microdepositional events (thin stringers) lower PC6
Early Holocene (~11,600–6,000)	Archaeological component(s)	CZ2	Lower CZ1b, CZ2 (undated)	n/a; Broken Mammoth– CZ1b, CZ2	n/a	Upper Component	n/a
	In-field pedostratigraphy	Silt deposition; C1	Silt deposition	Silt deposition; C	C1, Bwb, Ab1, C/B, PC1, C2, C3	Soil welding + "forest soil" formation; C4/Bwb4, C5Bwb5, C6, PC, Bwb6	Units: T1, PC2, PC1, PC0
	Micromorphology	-	Iron oxide mottling (in test pit)	-	-	Few pedofeatures; weak pedogenesis	Increased input of "woody" organic matter (PC1); micritic calcite features (PC1); evidence of soil formation (PC1); more pedofeatures than MH or LH;

(Continues)

TABLE 6 (Continued)

Time period (cal yr BP)	Scales of observation	Swan point	Mead	Camp	Keystone dune	Cook	Hurricane bluff
*Younger Dryas (~12,900–11,600)	Archaeological component(s)	CZ3a, CZ3b	CZ3	n/a; Broken Mammoth – CZ3	n/a	Lower Component	n/a
	In-field pedostratigraphy	Silt deposition, weak Ab horizons; C3/Ab3, C2/Ab2, Ab1	Upper Paleosol Complex (UPC)	Upper Paleosol/ Middle Paleosol Complexes	Weak soil formation + series of >16 Entisols; possible increase in wildfires; PC2, Ab2, Ab3, PC3, PC4, Ab4	Weakly developed Ab + Abk soil horizons; C7, PC	–
	Micromorphology	Localized freeze-thaw (platy + lenticular microstructures and fine-grain cappings) throughout mottled silt layers; no evidence of true pedogenesis; only "pseudo-soils" due to freeze-thaw	Evidence of soil formation + thicker Ab horizon within UPC; freeze-thaw (platy microstructure) below Ab horizon and fine-grain cappings; micritic calcite + redox features present; depositional events near lower boundary (abundant thin stringers)	High bioturbation and root disturbance; few pedofeatures	Microlaminations in Ab2 and Ab3; vertical grain size variations in PC3 and PC4	Very weak pedogenesis; few pedofeatures	–
*Bølling-Allerød (~14,000–12,900)	Archaeological component(s)	CZ4a, CZ4b	CZ4, CZ5	n/a; Broken Mammoth – CZ4a, CZ4b, CZ4c	Short-term occupation (hunting camp) + faunal remains	n/a	n/a
	In-field pedostratigraphy	C4, C5 = coarse silt/sands	Lower Paleosol Complex (LPC)	Lower Paleosol Complex	PC5	Undated (C8 below PC)	–
	Micromorphology	"pseudo-soil" development due to freeze-thaw	Groundwater rise between LPC and UPC; Depositional events at lower boundary (abundant thin stringers); micritic calcite + redox features present;	Subtle grain size variations; high bioturbation; weak micritic calcite pedofeatures present	Soil development (pedocomplex); vertical grain size variations; hydrologic fluctuation (mottling)	Higher energy deposition (Poor sorting, coarser grains)	–
References		Hirasawa and Holmes (2017)	Potter et al. (2011), Potter et al. (2013)	Dilley (1998); Holmes 1996	Lanoë et al. (2018); Reuther et al. (2016)	Reuther (2013)	Potter et al. (2007); Reuther et al. (2018)

Note: The "–" symbol indicates that either samples from the stratigraphic unit were not studied, or there are no notable features relevant to our major points in the main text. A "*" indicates that the Younger Dryas and Bølling-Allerød are part of the Late Glacial period.

based on the close association between hypocoatings and pore spaces (Figures 10, 11, and S23A–S23D), a diffuse, "halo-like" appearance (Figures 11a and S23B), and the lack of a decalcified zone around the hypocoatings (Figures 11a and S23B; Courty et al., 1989; Miller & Goldberg, 2009, p. 85; Sehgal & Stoops, 1972).

The presence of a sparitic calcite layer between the Lower Paleosol Complex and Upper Paleosol Complex indicates significant hydrologic change following Lower Paleosol Complex formation (Figures 11c,d and S21D). Sparitic calcite tends to form in the phreatic (groundwater) zone under longer periods of water saturation, which allows for larger crystal growth (Durand, Monger, & Canti, 2010; Miller & Goldberg, 2009). Therefore, we posit that this layer of sparitic calcite formed because of rising groundwater. A higher water table and prolonged saturation may have partially dissolved existing calcite pedofeatures in the Lower Paleosol Complex, as indicated by the rough, "dog-tooth" appearance of spar crystals and some hypocoatings.

In the Upper Paleosol Complex, we see a return to micritic calcite formation, indicating a lower water table and episodic wetting of the vadose zone (Gilbert, 2011; Potter et al., 2013). Contemporaneous calcium-rich layers are noted across the mTV (Dilley, 1998; Reuther, 2013). We also observe a similar temporal relationship between calcite and redoximorphic pedofeatures, as iron oxides consistently overprint calcite (Figures 10 and S22). Calcite features likely formed first through localized flow of soil water under generally drier conditions. Following calcite formation, iron oxide features formed around a younger root system, perhaps under wetter, cooler, and well-drained conditions. Quasi-coatings indicate a shift to free drainage at the site, rather than localized water movement through root pores (Lindbo, Stolt, & Vepraskas, 2010).

If soil moisture levels had frequently fluctuated during the Late Glacial, we would expect to see calcite and iron hypocoatings superimposed on each other (Goldberg & Holliday, 1998). Instead, we consistently observe iron pedofeatures overprinting calcite pedofeatures. Therefore, we hypothesize that Mead experienced a single, directional hydrologic and/or climatic shift during soil formation intervals of the Late Glacial.

5.3 | Do we observe evidence of stratigraphic and/ or landscape disturbance processes?

Bioturbation and cryoturbation are the most common landscape disturbance processes in the study region. In our samples, evidence of these disturbance mechanisms was either not present or only weakly expressed, consistent with previous observations (Dilley, 1998; Gilbert, 2011; Reuther, 2013). Bioturbation is primarily associated with modern root growth, although we do observe ancient root activity in buried A horizons. Animal bioturbation is less apparent, and the few observed passage features are not laterally or vertically extensive. Cryoturbation has clearly impacted these sites, but the effects of freeze-thaw processes are often weakly expressed or not extreme enough to disturb stratigraphy or archaeological

occupations (Dilley, 1998; Gilbert, 2011; Lanoë & Holmes, 2016; Potter et al., 2018). Our samples contain the greatest evidence of cryoturbation at Swan Point and Mead, limited evidence in the lowest stratigraphic units at Hurricane Bluff, and no evidence at Camp, Keystone Dune, or Cook. We posit that aspect and landform position best explain these trends. At Swan Point, our 1 × 1 m² test pit has a more northern aspect than the other sites and is sheltered from solar insolation by surrounding knolls. At Mead, our test pit has a local aspect that deviates slightly from south, a location set back from the bluff edge, and is sheltered by surrounding bluffs. By contrast, our other study sites have southern aspects and/or bluff edges fully exposed to solar radiation, so we would expect to see less evidence of freeze-thaw activity at these localities.

Bioturbation was most significant at the Camp section and Hurricane Bluff. One possible explanation is that both sites sit at the bluff edge; in this landscape position, sediments generally experience maximum drainage and temperatures, which results in heightened bioturbation (Thorson, 2006). At Camp, our analysis reveals extensive mixing of organic matter with different degrees of humification (i.e., from different time periods and potentially different sources) within the Middle and Lower Paleosol Complexes (Figure 8e). There is also some burrowing and significant modern root contamination of the original horizons, but these effects are easily discernible and traceable across a section. At Hurricane Bluff, we see similar mixing of organic matter in Pedocomplex 1 (Early Holocene) and Pedocomplex 6 (Middle Holocene). However, microlaminations and original bedding are preserved, suggesting that bioturbation is not significant enough to disturb stratigraphic integrity (Figure S24). At these two sites, bioturbation due to root growth is a concern for gathering paleoenvironmental proxy information and ensuring a "true" signal from the targeted horizon or stratigraphic unit. Future researchers must consider this when developing regional proxy records from individual sites.

At Swan Point, cryoturbation is strongly expressed in the 1 × 1 m² test pit, located in a poorly drained swale west of the main excavation. During fieldwork, we observed frozen ground at c. 100–140 cmbs in June 2016 and c. 50 cmbs on the north hillslope in June 2018, which provided clear evidence of poor drainage and seasonal freezing at this landform position. In test pit samples, we observe the incorporation of coarse quartz grains (Figure 4c,d), well-expressed ice-lensing and fine-grain cappings (Figure 5a–c, S20A, S20B), and incipient lenticular microstructure in the mottled sediment (Figure 5c). We also see platy and lenticular microstructure associated with Bw soil formation. Ice-lensing can result from several frost cycles within a single year, whereas platy and lenticular microstructures indicate "several generations of repetitive ice lensing" (Van Vliet-Lanoë, 2010, p. 89). Subhorizontal platy or lenticular structure is diagnostic of "deeply frozen loamy soils" (Schuman & Rieger, 2007, p. 27; Thorson, 1990, p. 405). Experiments indicate lenticular microstructure requires at least 18–25 freeze-thaw cycles to develop, whereas field observations suggest 100 or more cycles (Van Vliet-Lanoë, Coutard, & Pissart, 1984). At the test pit, our observations indicate numerous cycles of seasonal freezing throughout

the Late Glacial and into the Holocene. Local factors, such as aspect, shadiness, drainage, thickness of vegetative mat, and water saturation, may have played an important role in permafrost formation in this swale, as noted elsewhere in our study region (Thorson, 1990).

In contrast, the main excavation sequence at Swan Point exhibits little obvious evidence of freeze-thaw activity. We observe weak ice-lensing features in the lower Bw horizon, but the deeper sediments only give possible hints of cryoturbation, such as faint, dark brown bands observed in the field. As noted, these bands are potential "pseudo soils" that may be the result of freeze-thaw processes (Figure 5d). Microlaminations, grain size variations, and poor sorting could also be related to freeze-thaw processes (Figure 4). Frost-sorting and/or gelifluction are known mechanisms for concentrating coarse mineral grains, as observed in other high-latitude loess sections (Harris, 1985). Downward movement of the freezing plane can lead to upward movement of coarser material towards the surface, and a simultaneous downward migration of fine grains (Harris, 1985). The unexpected grain sorting in our thin sections warrants future investigation of cryoturbation at Swan Point.

At Mead, initial fieldwork suggested that lower cultural zones were unaffected by cryogenic processes (Dilley, 1998). However, previous micromorphological analysis (Gilbert, 2011) and our own results provide evidence for weak cryogenic disturbance in the Upper Paleosol Complex. We find platy microstructure just below a thicker Ab horizon in the upper portion of this paleosol complex, indicative of a deeply frozen soil (Thorson, 1990; Figures 5e,f and S20C). In the lower Upper Paleosol Complex, there are abundant fine-grain cappings on coarser mineral grains. Fine-grain cappings can result from water translocation during spring thaw and/or seasonal water perching above the active permafrost layer (Harris & Ellis, 1980; Tarnocai & Smith, 1989; Todisco & Bhiry, 2008). Signs of cryogenic processes are laterally continuous across the landform, extending from the upper slope to the bluff edge (main excavation profile). The Upper Paleosol Complex clearly experienced seasonal freezing, although archaeological components were likely not disturbed (Gilbert, 2011).

5.4 | Does micromorphology provide new insight on Late Glacial landscape evolution and paleoenvironmental reconstruction?

Our analysis provides new data on changes in local landscapes and environments during the Bølling-Allerød and Younger Dryas, as well as general trends during the Holocene. These data add to current paleoenvironmental reconstructions for our study sites.

During the Bølling-Allerød, we see the beginnings of landscape stabilization and reduced deposition compared to the Last Glacial Maximum (LGM, c. 20,000 cal yr BP; Dilley, 1998; Gilbert, 2011; Reuther, 2013). For example, a pedocomplex formed at Keystone Dune, and Mead experienced the formation of the thicker Lower Paleosol Complex during this interval. However, microlaminations and thin organic stringers within the Lower Paleosol Complex at Mead suggest that soil formation followed small-scale depositional events and/or local reworking of organic matter (Figures 6e,f, S21E, and S21F). We observe more organic stringers in the Lower Paleosol Complex than the Upper, suggesting a more dynamic local landscape in the Bølling-Allerød than the Younger Dryas. In terms of climate, existing records indicate climatic warming and increased moisture c. 14,000 to 13,500 cal yr BP (Bigelow & Edwards, 2001; Bigelow & Powers, 2001; Edwards, Mock, Finney, Barber, & Bartlein, 2001; Tinner et al., 2006). Increasing summer insolation and changing orbital parameters could have fostered permafrost melting in the spring and relatively warm, semiarid conditions in the summer (Berger, 1978; Bigelow & Powers, 2001). Our analysis provides support for warmer, semiarid conditions at the Mead site c. 13,400–13,200 cal yr BP, as indicated by abundant and well-developed micritic calcite hypocoatings. However, we note that changes in drainage and moisture input also shaped the local environment. Following an interval of greater aridity and calcite hypocoating development, local hydrological conditions shifted toward increased moisture input and enhanced drainage, which resulted in iron hypocoating formation. By the latter Bølling-Allerød (c. 13,000–12,800 cal yr BP), wetter conditions fostered rising groundwater and sparitic calcite formation.

During the Younger Dryas, orbital forcing led to colder winter temperatures and warmer summer temperatures (i.e., greater seasonal extremes), while a strong high-pressure system centered north of Alaska created warmer and drier conditions over much of the interior (Bartlein, Anderson, Edwards, & McDowell, 1991; Edwards et al., 2001). However, sites across central Alaska show variable responses to global forcing; a few sites register cooler temperatures and heightened aridity, while others indicate warmer, wetter conditions or a muted response (Bigelow & Edwards, 2001; Kokorowski, Anderson, Mock, & Lozhkin, 2008). Previous geoarchaeological work in SCF uses the abundance of pedogenic carbonate in Younger Dryas paleosols as evidence for arid climatic conditions (Dilley, 1998; Reuther, 2013). At Mead, micritic calcite hypocoatings in the Upper Paleosol Complex provide evidence for warm, arid conditions, a lowered water table, and well-drained soil during this interval. Below the upper Ab horizon, we find a thin subsurface Bkb horizon, indicating warm, relatively arid summer conditions (Figures S23A and S23B) Subtle climatic and/or hydrologic shifts could have fostered another interval of iron oxide hypocoating development. Platy microstructure is also present below the Ab horizon, providing evidence of colder winter conditions and repeated cycles of permafrost formation. Nearby at Swan Point, platy and lenticular microstructures, ice-lensing features, and fine-grain cappings provide evidence for seasonal freezing cycles in areas of lower topography and reduced drainage. However, these features are not present at the crest of the landform. This suggests that local factors (e.g., topographic position, vegetation thickness, drainage, aspect, shade) may have played a bigger role than regional factors in permafrost formation during this time period.

Our analysis of Keystone Dune samples offers important information about paleoecological processes that may have shaped the landscape during the Younger Dryas. Previous studies posit that the thin Entisols at this site were charred by heightened wildfire activity

(Reuther et al., 2016). However, we did not observe charcoal or microcharcoal in thin section. One possibility is that wildfires did not strongly influence soil formation at Keystone Dune and the surrounding landscape. Although a lack of charcoal in our thin sections does not preclude wildfire occurrence, we would expect to observe charcoal (even in small quantities) if Younger Dryas fire cycles strongly impacted vegetation and soils on the dune surface. Observed organic matter does not appear carbonized or burned, and instead looks humified and bioturbated, as one might expect within a typical Ab horizon. A second possibility is that these soil horizons exhibit dramatic lateral variability, and our samples missed areas of higher charcoal abundance related to wildfire cycles. At other sites in the SCF and the broader mTV region, microcharcoal is more abundant during this time period, supporting the hypothesis of increased wildfire activity (Reuther et al., 2016; Tinner et al., 2006). Testing these competing hypotheses requires more laterally continuous micromorphological sampling.

Our Holocene samples show different hydrological patterns as compared to our Late Glacial samples. At Swan Point, the lower Bw horizon (dated to c. 9,000 cal yr BP) exhibits weak ice-lensing features, suggesting conditions were cool and/or wet enough to initiate repeated permafrost formation. At Cook, soils experienced welding and other cryoturbation effects (Reuther, 2013). The presence of soil welding across SCF indicates that regional conditions were an important control for permafrost formation in the Holocene. By contrast, local controls seem to predominate during the Late Glacial. Additionally, iron oxide mottling at Mead provides evidence for water table fluctuation. This contrasts with the Late Glacial pattern of directional shifts in hydrology at the site level.

Finally, micromorphology provides insight on the degree of local landscape instability in the study region, even in the face of a general trend of landscape stabilization from the LGM to the Holocene. Over this period, ameliorating climate (e.g., warmer temperatures, increased moisture), and decreased wind intensity led to greater vegetation coverage, higher lake levels, and increased paludification, all of which contributed to reduced sediment sources (Abbott, Finney, Edwards, & Kelts, 2000; Bigelow & Powers, 2001; Dilley, 1998; Edwards et al., 2001; Jones & Yu, 2010; Reuther, 2013; Wooller et al., 2012). Together, these factors resulted in a broad trend of particle size fining upward in our stratigraphic profiles (Dilley, 1998). However, microscale textural changes were superimposed on this general trend, and these features vary from site-to-site. Local changes in sediment source exposure through various mechanisms, such as bluff erosion and destabilization or loss of vegetation through fire exposure, resulted in sporadic shifts from finer (silt) to coarser (fine to medium sand) aeolian particles at our sites. Such textural changes or microscale units cannot be correlated from site-to-site, as they are time-transgressive and not clearly related to regional or global climatic shifts. Instead, they seem to be the product of site-specific, local environmental conditions, as revealed by micromorphology.

6 | CONCLUSIONS

As shown here, micromorphology is a powerful technique for elucidating fine-scale aspects of site formation, pedogenic and depositional processes, landscape evolution, and postdepositional disturbance. This study demonstrates the great utility of micromorphological analysis at archaeological sites in central Alaska and in the subarctic more generally, where fine-scale features of soils and stratigraphy can be difficult to observe and describe in the field. In previous studies, this technique has been used at individual sites, often with emphasis on the archaeological stratigraphy (Blong & DiPietro, 2014; Gilbert, 2011; Graf et al., 2017, 2015; Josephs, 2010). Here we apply the technique at six sites, focusing on buried soils and pedostratigraphy. This study represents the first multisite, comparative analysis across the study region, with the goal of testing field interpretations about site formation and pedogenesis and improving current models of landscape evolution since the Late Glacial. We use the proximity of several early archaeological sites in SCF and the neighboring DRV as a natural laboratory to test hypotheses about soil formation, the effects of local versus regional environmental conditions, and processes responsible for site formation. This analysis provides a new perspective on landscape heterogeneity that we could not achieve without comparing many sites at the microscale.

While our findings generally support existing interpretations and paleoenvironmental records, micromorphology reveals microscale features that alter site formation models at some sites. Most importantly, we see microlaminations and depositional lenses within pedocomplexes at Mead and Hurricane Bluff. The surrounding organic-rich layers have previously been described as paleosols, but micromorphology indicates that depositional and/or freeze-thaw processes played a role in their formation. This analysis reveals a certain degree of landform and landscape instability, even in the face of regional increases in pedogenesis and vegetative coverage (e.g., shrub and forest expansions; Reuther, 2013). Researchers at subarctic sites must exercise caution when interpreting dark brown, organic-rich layers. We recommend testing interpretations with micromorphology whenever possible, as the presence of buried soils versus depositional stringers has different implications for reconstructing ancient landscapes.

Our analysis also highlights striking intersite differences in grain size variation, presence of bedding and microlaminations, microstructure, organic matter distribution, and pedofeature type and abundance. Such variability from site-to-site might be unexpected, given the proximity of these sites and broad stratigraphic similarities in the field. However, significant microscale variability in our analysis reinforces the hypothesis that localized landscape processes played a large role in shaping these sites (Lanoë et al., 2020; Reuther, 2013; Reuther et al., 2016). Our work provides a lesson in considering the significance of landscape heterogeneity in both paleoenvironmental interpretations and archaeological models of human ecology.

Going forward, micromorphology should play a prominent role in assessing stratigraphy at archaeological localities across the subarctic. By adding micromorphology to the repertoire, we can strengthen our hypotheses about past landscape change and possible human-environment

relationships in the far north. Future work should include: (a) thorough sampling at a given study site, with attention paid to both lateral and vertical variability, (b) comparing samples from archaeological profiles with samples from off-site, geologic profiles, to assess the impact of anthropogenic activities on sedimentological and pedogenic characteristics, and finally, (c) systematic sampling from different landscape positions to assess the impact of environmental factors such as drainage, slope position, vegetation coverage, proximity to sediment source, and geomorphology on observable characteristics. Soils, sediments, and landscape processes within periglacial and/or subarctic environments exhibit a variety of unique and often poorly understood characteristics. Systemic micromorphological analysis would address these gaps in our knowledge and enhance understanding of dynamic landscape evolution in this region.

DATA AVAILABILITY STATEMENT

The data that support the findings of this study are available from the corresponding author upon reasonable request.

ORCID

Jennifer Kielhofer http://orcid.org/0000-0001-9389-3570
Joshua Reuther https://orcid.org/0000-0002-3877-359X
Charles Holmes http://orcid.org/0000-0003-4422-2310
François Lanoë http://orcid.org/0000-0002-4627-140X

REFERENCES

Abbott, M. B., Finney, B. P., Edwards, M. E., & Kelts, K. R. (2000). Lake-level reconstructions and paleohydrology of Birch Lake, Central Alaska, based on seismic reflection profiles and core transects. *Quaternary Research*, 53(2), 154–166. https://doi.org/10.1006/qres.1999.2112

Bartlein, P. J., Anderson, P. M., Edwards, M. E., & McDowell, P. F. (1991). A framework for interpreting paleoclimatic variations in Eastern Beringia. *Quaternary International*, 10–12(C), 73–83. https://doi.org/10.1016/1040-6182(91)90041-L

Berger, A. L. (1978). Long-term variations of caloric insolation resulting from Earth's orbital elements. *Quaternary Research*, 9, 139–167.

Bigelow, N. H., & Edwards, M. E. (2001). A 14,000 yr paleoenvironmental record from Windmill Lake, central Alaska: Lateglacial and Holocene vegetation in the Alaska range. *Quaternary Science Reviews*, 20(1–3), 203–215. https://doi.org/10.1016/S0277-3791(00)00122-0

Bigelow, N. H., & Powers, W. R. (2001). Climate, vegetation, and archaeology 14,000–9,000 cal yr B.P. in central Alaska. *Arctic Anthropology*, 38(2), 171–195.

Blong, J. C., & DiPietro, L. M. (2014). Stratigraphy, dating, and lithic assemblages from Middle to Late Holocene sites in the Ewe Creek Drainage, Denali National Park and Preserve. *Alaska Journal of Anthropology*, 12(2), 74–90.

Courty, M. A. (2001). Microfacies analysis assisting archaeological stratigraphy. In V. T. Paul Goldberg, Holliday & C. R. Ferring (Eds.), *Earth sciences and archaeology* (pp. 205–239). New York, NY: Kluwer Academic/Plenum Publishers. https://doi.org/10.2223/JPED.2079

Courty, M. A., Goldberg, P., & Macphail, R. I. (1989). *Soils and micromorphology in archaeology*. Cambridge: Cambridge University Press.

Dilley, T. R. (1998). *Late Quaternary loess stratigraphy, soils, and environments of the Shaw Creek Flats Paleoindian sites, Tanana Valley, Alaska* (Dissertation). University of Arizona. https://doi.org/10.1016/j.jorganchem.2010.09.058

Durand, N., Monger, C. H., & Canti, M. G. (2010). Calcium carbonate features. In G. Stoops, V. Marcelino & F. Mees (Eds.), *Interpretation of micromorphological features of soils and regoliths* (pp. 149–194). Amsterdam: Elsevier B.V. https://doi.org/10.1016/B978-0-444-53156-8.00009-X

Edwards, M. E., Mock, C. J., Finney, B. P., Barber, V. A., & Bartlein, P. J. (2001). Potential analogues for paleoclimatic variations in eastern interior Alaska during the past 14,000 yr: Atmospheric-circulation controls of regional temperature and moisture responses. *Quaternary Science Reviews*, 20(1–3), 189–202. https://doi.org/10.1016/S0277-3791(00)00123-2

Gilbert, P. J. (2011). *Micromorphology, Site Spatial Variation and Patterning, and Climate Change at the Mead Site (XBD-071): A Multi-Component Archaeological Site in Interior Alaska*. Fairbanks: University of Alaska. https://doi.org/10.1080/01402390.2011.569130

Goldberg, P. (2000). Micromorphology and site formation at Die Kelders Cave I, South Africa. *Journal of Human Evolution*, 38(1), 43–90. https://doi.org/10.1006/jhev.1999.0350

Goldberg, P., & Holliday, V. T. (1998). Geology and Stratigraphy. In M. B. Collins, G. L. Bailey, C. B. Bousman, S. W. Dial, P. Goldberg, J. Guy & P. R. Takac (Eds.), *Wilson-Leonard: An 11,000-year archaeological record of hunter-gatherers in central Texas. Volume 1: Introduction, background, and syntheses* (pp. 77–121). Austin, TX: The University of Texas.

Gómez Coutouly, Y. A., & Holmes, C. E. (2018). The microblade industry from Swan Point Cultural Zone 4b: Technological and cultural implications from the earliest human occupation in Alaska. *American Antiquity*, 83(4), 735–752. https://doi.org/10.1017/aaq.2018.38

Graf, K. E., DiPietro, L. M., Krasinski, K. E., Culleton, B. J., Kennett, D. J., Gore, A. K., & Smith, H. L. (2017). New geoarchaeology and geochronology at Dry Creek. In T. Goebel (Ed.), *Dry Creek: archaeology and paleoecology of a late Pleistocene hunting camp*, First ed., (pp. 219–260). College Station, TX: Texas A&M University Press.

Graf, K. E., DiPietro, L. M., Krasinski, K. E., Gore, A. K., Smith, H. L., Culleton, B. J., & Rhode, D. (2015). Dry creek revisited: New excavations, radiocarbon dates, and site formation inform on the peopling of eastern Beringia. *American Antiquity*, 80(04), 671–694. https://doi.org/10.7183/0002-7316.80.4.671

Guthrie, R. D. (1990). *Frozen fauna of the mammoth steppe: The story of blue babe*. Chicago, IL: The University of Chicago Press.

Harris, C. (1985). Geomorphological applications of soil micromorphology with particular reference to periglacial sediments and processes. In K. S. Richards, R. R. Arnett, S. Ellis & B. G. R. Group (Eds.),

Geomorphology and soils (pp. 219–232). London and Boston, MA: G. Allen & Unwin.

Harris, C., & Ellis, S. (1980). Micromorphology of soils in soliflucted materials, Okstindan, Northern Norway. *Geoderma, 23*(1), 11–29. https://doi.org/10.1016/0016-7061(80)90046-4

Hirasawa, Y., & Holmes, C. E. (2017). The relationship between microblade morphology and production technology in Alaska from the perspective of the Swan Point site. *Quaternary International, 442,* 104–117. https://doi.org/10.1016/j.quaint.2016.07.021

Hoffecker, J. F., & Elias, S. A. (2007). *Human ecology of Beringia.* New York: Columbia University Press. https://doi.org/10.7312/hoff13060

Holmes, C. E. (2001). Tanana River Valley archaeology circa 14,000 to 9000 B.P. *Arctic Anthropology, 38*(2), 154–170.

Holmes, C. E. (2011). The beringian and transitional periods in Alaska: Technology of the East Beringian tradition as viewed from Swan Point. In T. Goebel & I. Buvit (Eds.), *From the Yenisei to the Yukon: Interpreting lithic assemblage variability in the late Pleistocene/early Holocene Beringia* (1st ed., pp. 179–191). College Station, TX: A&M University Press.

Jones, M. C., & Yu, Z. (2010). Rapid deglacial and early Holocene expansion of peatlands in Alaska. *Proceedings of the National Academy of Sciences of the United States of America, 107*(16), 7347–7352. https://doi.org/10.1073/pnas.0911387107

Josephs, R. L. (2010). Micromorphology of an Early Holocene Loess-Paleosol Sequence, Central Alaska, U.S.A. *Arctic, Antarctic, and Alpine Research, 42*(1), 67–75. https://doi.org/10.1657/1938-4246-42.1.67

Josephs, R. L., & Bettis, E. A. (2003). Short contribution: A practical alternative to Kubiena boxes for the collection of samples for micromorphological analysis. *Geoarchaeology, 18*(5), 567–570. https://doi.org/10.1002/gea.10075

Kokorowski, H. D., Anderson, P. M., Mock, C. J., & Lozhkin, A. V. (2008). A re-evaluation and spatial analysis of evidence for a Younger Dryas climatic reversal in Beringia. *Quaternary Science Reviews, 27*(17–18), 1710–1722. https://doi.org/10.1016/j.quascirev.2008.06.010

Lanoë, F. B. (2018). *Faunal analysis report Swan Point (XBD-156).*

Lanoë, F. B., & Holmes, C. E. (2016). Animals as raw material in Beringia: Insights from the site of Swan Point CZ4B, Alaska. *American Antiquity, 81*(4), 682–696.

Lanoë, F. B., Reuther, J. D., Holloway, C. R., Holmes, C. E., & Kielhofer, J. R. (2018). The Keystone Dune Site, A Bølling-Allerød Hunting Camp in Eastern Beringia. *PaleoAmerica, 4,* 151–161.

Lanoë, F. B., Reuther, J. D., & Holmes, C. E. (2018). Task-Specific Sites and Paleoindian Landscape Use in the Shaw Creek Flats, Alaska. *Journal of Archaeological Method and Theory, 25,* 818–838. https://doi.org/10.1007/s10816-017-9360-0

Lanoë, F. B., Reuther, J. D., Holmes, C. E., & Potter, B. A. (2020). Small mammals and paleoenvironmental context of the terminal pleistocene and early holocene human occupation of central Alaska. *Geoarchaeology, 35,* 164–176. https://doi.org/10.1002/gea.21768

Lindbo, D. L., Stolt, M. H., & Vepraskas, M. J. (2010). Redoximorphic features. In G. Stoops, V. Marcelino & F. Mees (Eds.), *Interpretation of Micromorphological Features of Soils and Regoliths,* 1st ed, (pp. 129–147). Amsterdam: Elsevier B.V. https://doi.org/10.1016/B978-0-444-53156-8.00008-8

Matmon, A, Briner, J. P., Carver, G., Bierman, P., & Finkel, R. C. (2010). Moraine chronosequence of the Donnelly Dome region, Alaska. *Quaternary Research, 74*(1), 63–72. https://doi.org/10.1016/j.yqres.2010.04.007

Miller, C. E., & Goldberg, P. (2009). Micromorphology and paleoenvironments. M. L. Larson M. Kornfeld & G. C. Frison *Hell Gap: A Paleoindian Campsite at the Edge of the Rockies,* 72–89. Salt Lake City. University of Utah Press.

Muhs, D. R., Ager, T. A., Bettis, E. A., McGeehin, J., Been, J. M., Begét, J. E., & Stevens, D. A. S. P. (2003). Stratigraphy and palaeoclimatic significance of Late Quaternary loess-palaeosol sequences of the Last Interglacial-Glacial cycle in central Alaska. *Quaternary Science Reviews, 22*(18–19), 1947–1986. https://doi.org/10.1016/S0277-3791(03)00167-7

Péwé, T. L. (1965). Middle Tanana River Valley. *Central and South-Central Alaska: Guidebook for Field Conference* (pp. 36–54).

Péwé, T. L., & Reger, R. D. (1983). *Richardson and Glenn Highways, Alaska: Guidebook to Permafrost and Quaternary Geology.* Fairbanks.

Péwé, T. L., & Reger, R. D. (1993). *Guidebook to permafrost and Quaternary geology along the Richardson and Glenn Highways between Fairbanks and Anchorage, Alaska.*

Ping, C. L., Michaelson, G. J., Packee, E. C., Stiles, C. A., Swanson, D. K., & Yoshikawa, K. (2005). Soil catena sequences and fire ecology in the boreal forest of Alaska. *Soil Science Society of America Journal, 69*(6), 1761–1772. https://doi.org/10.2136/sssaj2004.0139

Potter, B. A. (2005). Site structure and organization in Central Alaska: Archaeological investigations at Gerstle River [dissertation]. *University of Alaska Fairbanks.*

Potter, B. A. (2009). Tanana River Basin, East Central Alaska: Understanding Colonization of the New World. F. P. McManamon L. S. Cordell K. Lightfoot & G. R. Milner *Archaeology in America.*West Coast and Arctic/Subarctic4, 308–310). Westport, CT and London: Greenwood Press.

Potter, B. A., Bowers, P. M., Reuther, J. D., & Mason, O. K. (2007). Holocene assemblage variability in the Tanana Basin: NLUR archaeological research, 1994–2004. *Alaska Journal of Anthropology, 5*(1), 23–42.

Potter, B. A., Esdale, J. A., Reuther, J. D., McKinney, H. J., Holmes, C. E., Holloway, C. R., & Glassburn, C. L. (2018). *Archaeological investigations at Delta River overlook, Central Alaska.* Fairbanks.

Potter, B. A., Gilbert, P. J., Holmes, C. E., & Crass, B. A. (2011). The Mead Site, a Late-Pleistocene/Holocene Stratified Site in Central Alaska. *Current Research in the Pleistocene, 28,* 73–75.

Potter, B. A., Holmes, C. E., & Yesner, D. R. (2013). Technology and economy among the earliest prehistoric foragers in Interior Eastern Beringia. In K. E. Graf, C. V. Ketron, & M. R. Waters (Eds.), *Paleoamerican Odyssey* (pp. 81–103). College Station: Texas A&M University Press.

Potter, B. A., Irish, J. D., Reuther, J. D., Gelvin-Reymiller, C., & Holliday, V. T. (2011). A Terminal Pleistocene child cremation and residential structure from Eastern Beringia. *Science, 331*(6020), 1058–1062. https://doi.org/10.1126/science.1201581

Reger, R. D., & Péwé, T. L. (2002). *Geologic map of the Big Delta A-4 quadrangle, Alaska* (Alaska Division of Geological & Geophysical Surveys Report of Investigation 2002-2, 1 sheet, scale 1:63,360). Fairbanks.

Reger, R. D., & Solie, D. N. (2008). *Reconnaissance Interpretative of Permafrost, Alaska Highway Corridor, Delta Junction to Dot Lake, Alaska.* Fairbanks.

Reger, R. D., Stevens, D. A. S. P., & Solie, D. N. (2008). *Surficial geology of the Alaska Highway corridor, Delta Junction to Dot Lake, Alaska.* Fairbanks.

Reuther, J. D. (2013). *Late Glacial and Early Holocene geoarchaeology and terrestrial paleoecology in the lowlands of the middle Tanana Valley, subarctic Alaska* [dissertation]. University of Arizona. https://doi.org/10.1016/j.talanta.2008.12.059

Reuther, J. D., Potter, B. A., Holmes, C. E., Feathers, J. K., Lanoë, F. B., & Kielhofer, J. R. (2016). The Rosa-Keystone Dunes Field: The geoarchaeology and paleoecology of a late Quaternary stabilized dune field in Eastern Beringia. *The Holocene, 26*(12), 1939–1953. https://doi.org/10.1177/0959683616646190

Reuther, J. D., Potter, B. A., Mulliken, K. M., & Kielhofer, J. R. (2018). Geoarchaeology—Delta River ōverlook and Hurricane Bluff sites. In B. A. Potter, J. A. Esdale, J. D. Reuther, H. J. McKinney, C. E. Holmes, C. R. Holloway & C. L. Glassburn (Eds.), *Archaeological investigations at Delta River overlook, Central Alaska. Archaeology GIS Laboratory, Report #7* (pp. 72–141). Fairbanks: University of Alaska Fairbanks, Department of Anthropology.

Rieger, S., Schoephorster, D. B., & Furbush, C. E. (1979). *Exploratory soil survey of Alaska.* Washington D.C.: U.S. Department of Agriculture, Soil Conservation Service.

Schuman, G. E., & Rieger, S. (2007). The genesis and classification of cold soils (Vol. 37). New York, NY: Academic Press. https://doi.org/10.2307/3898860

Sehgal, J. L., & Stoops, G. (1972). Pedogenic calcite accumulation in arid and semi-arid regions of the Indo-Gangetic alluvial plain of Erstwhile Punjab (India)—Their morphology and origin. *Geoderma*, 8, 59–72.

Stoops, G. (2003). In (Ed.), *Guidelines for analysis and description of soil and regolith thin sections*. Madison, WI: Soil Science Society of America, Inc.

Stoops, G., Marcelino, V. & Mees, F. (Eds.), (2010). *Interpretation of micromorphological features of soils and regoliths*, 1st ed. Amsterdam: Elsevier B.V.

Stuiver, M., Reimer, P. J., & Reimer, R. W. (2019). Calib 7.1 (WWW program). Retrieved from http://calib.org

Tarnocai, C., & Smith, C. A. S. (1989). Micromorphology and development of some central Yukon paleosols, Cananda. *Geoderma*, 45(89), 145–162.

Ten Brink, N. W., & Waythomas, C. F. (1980). *Late Wisconsin glacial chronology of the north-central Alaska Range—A regional synthesis and its implications for early human settlements. North Alaska Range Project: Preliminary progress report on 1978 and 1979 geoarchaeological studies.*

Thorson, R. M. (1990). Geologic contexts of archaeological sites in Beringia. In N. P. Lasca & J. Donahue (Eds.), *Archaeological Geology of North America* (pp. 399–420). Boulder, CO: Geological Society of America. Centennial.

Thorson, R. M. (2006). Artifact mixing at the Dry Creek site, interior Alaska. *Anthrological Papers of the University of Alaska New Series*, 4, 1–10.

Thorson, R. M., & Hamilton, T. D. (1977). Geology of the Dry Creek site: A stratified early man site in Interior Alaska. *Quaternary Research*, 7(2), 149–176. https://doi.org/10.1016/0033-5894(77)90034-5

Thorson, R. M., & Tryon, C. A. (2003). Bluff top sand sheets in northeastern archaeology: A physical transport model and application to the Neville site, Amoskeag Falls, New Hampshire. In D. L. Cremeens & J. P. Hart (Eds.), *Geoarchaeology of Landscapes in the Glaciated Northeast* (pp. 61–73). New York, NY: Albany: University of the State of New York.

Tinner, W., Hu, F. S., Beer, R., Kaltenrieder, P., Scheurer, B., & Krähenbühl, U. (2006). Postglacial vegetational and fire history: Pollen, plant macrofossil and charcoal records from two Alaskan lakes. *Vegetation History and Archaeobotany*, 15(4), 279–293. https://doi.org/10.1007/s00334-006-0052-z

Todisco, D., & Bhiry, N. (2008). Micromorphology of periglacial sediments from the Tayara site, Qikirtaq Island, Nunavik (Canada). *Catena*, 76(1), 1–21. https://doi.org/10.1016/j.catena.2008.08.002

Van Vliet-Lanoë, B. (2010). Frost action. In G. Stoops, Marcelino & F. Mees (Eds.), *Interpretation of Micromorphological Features of Soils and Regoliths*, 1st ed, (pp. 81–108). Amsterdam: Elsevier B.V. https://doi.org/10.1016/B978-0-444-53156-8.00006-4

Van Vliet-Lanoë, B., Coutard, J. P., & Pissart, A. (1984). Structures caused by repeated freezing and thawing in various loamy sediments: A comparison of active, fossil and experimental data. *Earth Surface Processes and Landforms*, 9(6), 553–565. https://doi.org/10.1002/esp.3290090609

Wooller, M. J., Kurek, J., Gaglioti, B. V., Cwynar, L. C., Bigelow, N. H., Reuther, J. D., & Smol, J. P. (2012). An ~11,200 year paleolimnological perspective for emerging archaeological findings at Quartz Lake, Alaska. *Journal of Paleolimnology*, 48(1), 83–99. https://doi.org/10.1007/s10933-012-9610-9

Wygal, B. T., Krasinski, K. E., Holmes, C. E., & Crass, B. A. (2018). Holzman south: A Late Pleistocene archaeological site along Shaw Creek, Tanana Valley, Interior Alaska. *PaleoAmerica*, 4(1), 90–93. https://doi.org/10.1080/20555563.2017.1408358

Yesner, D. R. (1996). Human adaptation at the Pleistocene—Holocene boundary (ca 13,000–8,000 B.P.) in eastern Beringia. L. G. Straus B. V. Eriksen J. M. Erlandson & D. R. Yesner *Humans at the End of the Ice Age: The Archaeology of the Pleistocene-Holocene Transition*, Interdisciplinary Contributions to Archaeology, 255–276). Boston: .Springer.

SUPPORTING INFORMATION

Additional supporting information may be found online in the Supporting Information section.